Chapter 7
Interaction of Acoustic and Electromagnetic Waves

7.1 INTRODUCTION

As we have seen, acoustic waves propagate in an anisotropic medium as three distinct modes that are generally neither parallel nor perpendicular to the propagation direction. The symmetry properties of the crystal determine the propagation characteristics, including the phase velocity, polarization, and power flow angle. Similarly, understanding the propagation of electromagnetic waves in anisotropic crystals requires a knowledge of the symmetry properties of the medium and is generally more involved than propagation in an isotropic body. An added complication in the discussion of optic wave propagation is that many crystals absorb strongly in the visible band (wavelengths of 4000 to 7000 Å). For example, germanium, gallium arsenide, and other potentially useful crystals are opaque in the visible band. Furthermore, most materials exhibit *dispersion*, so a complete description requires that the permittivity matrix possess components that are complex and frequency dependent. In our discussion, we will assume that all permittivity components are real and nondispersive. Dispersion is included by specifying the permittivity components at a given optic wavelength.

In this chapter, we investigate the propagation of optic modes in anisotropic crystals, using the formalism developed in Chapter 2 for acoustic modes. The acoustic propagation properties are determined by the 6×6 symmetric stiffness matrix, but the electromagnetic propagation characteristics are determined by the 3×3 symmetric permittivity matrix. This fact and the form of the Maxwell equations lead to a somewhat simpler form for the electromagnetic modes. Instead of three modes, there are only two; both modes are shear, and one is always pure. Even in the

orthorhombic system, the phase velocity of the quasishear mode has an elliptic shape similar to the shape of the pure shear mode in the principal planes.

Electric and mechanical fields cause perturbations in the acoustic propagation in much the same way piezoelectricity perturbs acoustic propagation. Unlike piezoelectricity, which changes only the stiffness components (not the form of the stiffness matrix), external fields change the symmetry properties of the medium causing, e.g., an isotropic medium to become uniaxial or even biaxial. Finally, we discuss the interaction of an optic mode with a high frequency acoustic wave. In this case, the direction and frequency of the optic beam are changed by the acoustic perturbation.

7.2 ELECTROMAGNETIC WAVES IN AN ANISOTROPIC MEDIUM

Our first goal is to write the Maxwell equation in a form similar to (2.40) and (2.41) and to develop an "optical" Christoffel equation. We write Faraday's law in its differential form:

$$\nabla \times \mathbf{E} = -\frac{\partial \mathbf{B}}{\partial t} \tag{7.1}$$

In Cartesian coordinates, the curl is

$$\nabla \times \mathbf{E} = \left(\frac{\partial E_z}{\partial y} - \frac{\partial E_y}{\partial z}\right)\hat{\mathbf{i}} + \left(\frac{\partial E_x}{\partial z} - \frac{\partial E_z}{\partial x}\right)\hat{\mathbf{j}} + \left(\frac{\partial E_y}{\partial x} - \frac{\partial E_x}{\partial y}\right)\hat{\mathbf{k}} \tag{7.2}$$

Equation (7.2) can be written in matrix format as

$$\nabla \times \mathbf{E} = \begin{vmatrix} \hat{\mathbf{i}} & \hat{\mathbf{j}} & \hat{\mathbf{k}} \\ \dfrac{\partial}{\partial x} & \dfrac{\partial}{\partial y} & \dfrac{\partial}{\partial z} \\ E_x & E_y & E_z \end{vmatrix} \tag{7.3}$$

We assume that the electric field varies sinusoidally with position:

$$\mathbf{E} \rightarrow e^{-jk\hat{\mathbf{l}}\cdot\mathbf{r}} = e^{-jk(l_x x + l_y y + l_z z)}$$

The derivatives take the form of operators:

$$\frac{\partial}{\partial x} \rightarrow -jkl_x, \frac{\partial}{\partial y} \rightarrow -jkl_y, \frac{\partial}{\partial z} \rightarrow -jkl_z$$

Equation (7.3) becomes

$$\nabla \times \mathbf{E} = -jk \begin{vmatrix} \hat{\mathbf{i}} & \hat{\mathbf{j}} & \hat{\mathbf{k}} \\ l_x & l_y & l_z \\ E_x & E_y & E_z \end{vmatrix} \tag{7.4}$$

Finally, we can write (7.4) as a *matrix* $\mathbf{l}$ operating on the vector $\mathbf{E}$ (compare this formulation with the gradient operator of (1.85)):

$$\nabla \times \mathbf{E} = \mathbf{l}:\mathbf{E} = jk \begin{bmatrix} 0 & -l_z & l_y \\ l_z & 0 & -l_x \\ -l_y & l_x & 0 \end{bmatrix} \begin{bmatrix} E_x \\ E_y \\ E_z \end{bmatrix} \tag{7.5}$$

Notice that $\mathbf{l}$ is a 3×3 antisymmetric matrix operator. For example, the x component of (7.5) is

$$(\nabla \times \mathbf{E})_x = -jk(-l_z E_y + l_y E_z) = \left(\frac{\partial E_z}{\partial y} - \frac{\partial E_y}{\partial z}\right)$$

Now, recall the wave equation for electromagnetic waves (4.35):

$$\nabla \times \nabla \times \mathbf{E} = -\mu\boldsymbol{\epsilon}:\frac{\partial^2 \mathbf{E}}{\partial t^2}$$

where we have allowed the permittivity $\boldsymbol{\epsilon}$ to be a (3×3) matrix, and we assume a nonmagnetic material so that the permeability is

$$\mu = \mu_0 = 4\pi \times 10^{-7}\ \text{H/m}$$

and, us usual;

$$\mathbf{B} = \mu_0 \mathbf{H}$$

Using the $\mathbf{l}$ operator matrices, we obtain from (7.5):

$$\begin{aligned} \nabla \times \nabla \times \rightarrow (\mathbf{l})^2 &= -k^2 \begin{bmatrix} 0 & -l_z & l_y \\ l_z & 0 & -l_x \\ -l_y & l_x & 0 \end{bmatrix} \begin{bmatrix} 0 & -l_z & l_y \\ l_z & 0 & -l_x \\ -l_y & l_x & 0 \end{bmatrix} \\ &= -k^2 \begin{bmatrix} -l_z^2 - l_y^2 & l_x l_y & l_x l_z \\ l_x l_y & -l_z^2 - l_x^2 & l_y l_z \\ l_x l_z & l_y l_z & -l_x^2 - l_y^2 \end{bmatrix} \end{aligned} \tag{7.6}$$

The wave equation for the electric field in an anisotropic crystal takes the form:

$$k^2\hat{\mathbf{l}}^2:\mathbf{E} - \omega^2\mu\boldsymbol{\epsilon}:\mathbf{E} = 0 \tag{7.7}$$

where now $\boldsymbol{\epsilon}$ is a 3×3 symmetric matrix (the symmetry of $\boldsymbol{\epsilon}$ like that of $\mathbf{c}$ follows from energy considerations):

$$\boldsymbol{\epsilon} = \begin{bmatrix} \epsilon_{11} & \epsilon_{12} & \epsilon_{13} \\ \epsilon_{12} & \epsilon_{22} & \epsilon_{23} \\ \epsilon_{13} & \epsilon_{23} & \epsilon_{33} \end{bmatrix} \tag{7.8}$$

Substituting (7.6) and (7.8) into (7.7), we have

$$\begin{bmatrix} -(l_y^2 + l_z^2) & l_x l_y & l_x l_z \\ l_x l_y & -(l_x^2 + l_z^2) & l_y l_z \\ l_x l_z & l_y l_z & -(l_x^2 + l_y^2) \end{bmatrix} \begin{bmatrix} E_x \\ E_z \\ E_z \end{bmatrix}$$

$$+ \omega^2\mu \begin{bmatrix} \epsilon_{11}E_x + \epsilon_{12}E_y + \epsilon_{13}E_z \\ \epsilon_{12}E_x + \epsilon_{22}E_y + \epsilon_{23}E_z \\ \epsilon_{13}E_x + \epsilon_{23}E_y + \epsilon_{33}E_z \end{bmatrix} = 0 \tag{7.9}$$

Equation (7.9) can also be written in the form:

$$\begin{bmatrix} -(l_x^2 + l_y^2) + \dfrac{\omega^2}{k^2}\mu\epsilon_{11} & l_x l_y + \dfrac{\omega^2}{k^2}\mu\epsilon_{12} & l_x l_z + \dfrac{\omega^2}{k^2}\mu\epsilon_{13} \\ l_x l_y + \dfrac{\omega^2}{k^2}\mu\epsilon_{12} & -(l_x^2 + l_z^2) + \dfrac{\omega^2}{k^2}\mu\epsilon_{22} & l_y l_z + \dfrac{\omega^2}{k^2}\mu\epsilon_{23} \\ l_x l_z + \dfrac{\omega^2}{k^2}\mu\epsilon_{13} & l_y l_z + \dfrac{\omega^2}{k^2}\mu\epsilon_{23} & -(l_x^2 + l_y^2) + \dfrac{\omega^2}{k^2}\mu\epsilon_{33} \end{bmatrix} \begin{bmatrix} E_x \\ E_y \\ E_z \end{bmatrix} = 0 \tag{7.10}$$

Equation (7.9) is the optic analogue of the Christoffel equation (2.48) and consists of the propagation matrix, which depends on $\hat{\mathbf{l}}$, a matrix that defines the symmetrical properties of the material, ϵ, and a field vector $\mathbf{E}$. Like the Christoffel matrix, the propagation matrix for electromagnetic waves is symmetric. In the form of (7.10), it contains the frequency and propagation constant terms explicitly, because in the acoustic wave equation the stiffness matrix is included in the gradient and divergence operator matrices (the spatial derivatives), whereas in the electromagnetic case the permittivity matrix is included in the time derivatives.

The components of the permittivity matrix define the propagation characteristics of the electromagnetic wave, as compared with the components of the stiffness matrix, which determined the propagation of acoustic waves. Because the permittivity is a symmetric 3×3 matrix, the maximum number of independent components is six. The number of independent components depends on the symmetry class. Equation (7.10) defines the propagation characteristics for the most general symmetry (triclinic), which contains all six independent permittivity components. Although it is, in principle, possible to write the (acoustic) Christoffel matrix for the triclinic symmetry, its form would be quite complex. For symmetry classes containing fewer independent components, the form of (7.10) remains the same but some of the permittivity terms vanish. A comparison of the stiffness and permittivity matrices is given in Table 7.1.

Table 7.1 Number of Independent Components

Symmetry Class	*Permittivity Matrix* $\boldsymbol{\epsilon}$	*Stiffness Matrix* $\mathbf{c}$
Isotropic	1 $\epsilon_{11} = \epsilon_{22} = \epsilon_{33}$ $e_{ij} = 0,\ i \neq j$	2
Cubic	1 (same as isotropic)	3
Hexagonal	2 $\epsilon_{11} = \epsilon_{22}$ $\epsilon_{ij} = 0,\ i \neq j$	5
Tetragonal	2 (same as hexagonal)	6 or 7 (dependent on class)
Trigonal	2 (same as hexagonal)	6 or 7 (dependent on class)
Orthorhombic	3 $\epsilon_{ij} = 0,\ i \neq j$	9
Monoclinic	4 $\epsilon_{12} = 0$	13
Triclinic	6	21

Because we consider only symmetry classes up to the orthorhombic class, we require that $\boldsymbol{\epsilon}$ be diagonal. In the monoclinic and triclinic symmetries, $\boldsymbol{\epsilon}$ can be put into diagonal form by a symmetry transformation (a rotation of coordinates). An important simplification in $\boldsymbol{\epsilon}$ over $\mathbf{c}$ is that

the cubic symmetry is optically isotropic. The reason is that the "rank" of $\boldsymbol{\epsilon}$ (3×3) is lower than the rank of $\mathbf{c}$ (6×6). Thus, if the three principal axes have the same value of permittivity (e.g., ϵ_{11}), then the projection of this value onto any other direction is also ϵ_{11} and the matrix collapses to a scalar.

We now consider propagation in the xy plane. If we assume that the permittivity is diagonal, (7.10) reduces to

$$(\epsilon_{11}\epsilon_{22}\epsilon_{33}) \begin{bmatrix} \dfrac{-l_y^2}{\epsilon_{22}\epsilon_{33}} + \mu\dfrac{\omega^2}{k^2} & \dfrac{l_x l_y}{\epsilon_{11}\epsilon_{22}\epsilon_{33}} & 0 \\ \dfrac{l_x l_y}{\epsilon_{11}\epsilon_{22}\epsilon_{33}} & \dfrac{-l_x^2}{\epsilon_{11}\epsilon_{33}} + \mu\dfrac{\omega^2}{k^2} & 0 \\ 0 & 0 & \dfrac{-(l_x^2 + l_y^2)}{\epsilon_{11}\epsilon_{22}} + \mu\dfrac{\omega^2}{k^2} \end{bmatrix} \begin{bmatrix} E_x \\ E_y \\ E_z \end{bmatrix} = 0 \quad (7.11)$$

The upper-left position of the Christoffel matrix (corresponding to an x-polarized acoustic wave) always contains a component of the propagation direction l_x multiplied by c_{11}, which corresponds to the longitudinal mode. As a consequence of the curl relations in (7.6), the upper-left position of (7.11) does not contain an l_x propagation component, and thus longitudinal modes are not present in electromagnetic waves. For an x-propagating wave, (7.11) reduces to

$$\begin{bmatrix} \dfrac{\omega^2}{k^2}\mu & 0 & 0 \\ 0 & \dfrac{-1}{\epsilon_{22}} + \mu\dfrac{\omega^2}{k^2} & 0 \\ 0 & 0 & \dfrac{-1}{\epsilon_{33}} + \mu\dfrac{\omega^2}{k^2} \end{bmatrix} \begin{bmatrix} E_x \\ E_y \\ E_z \end{bmatrix} = 0 \quad (7.12)$$

There are two propagating waves, one polarized in the y direction and one in the z direction, with velocities,

$$v_p = -\frac{1}{\sqrt{\mu\epsilon_{22}}} \qquad (E_y\text{-polarized wave})$$

$$v_p = \frac{1}{\sqrt{\mu\epsilon_{33}}} \qquad (E_z\text{-polarized wave})$$

Both waves are (in acoustic terminology) pure shear waves because they are polarized normal to the direction of propagation.

Similarly, for y- and z-propagating waves, we can easily find the two orthogonally polarized waves:

y-propagating:

$$v_p = \frac{1}{\sqrt{\mu\epsilon_{11}}} \qquad (E_x\text{-polarized})$$

$$v_p = \frac{1}{\sqrt{\mu\epsilon_{33}}} \qquad (E_z\text{-polarized})$$

z-propagating:

$$v_p = \frac{1}{\sqrt{\mu\epsilon_{11}}} \qquad (E_x\text{-polarized})$$

$$v_p = \frac{1}{\sqrt{\mu\epsilon_{22}}} \qquad (E_y\text{-polarized})$$

For cubic and isotropic symmetries:

$$\epsilon_{11} = \epsilon_{22} = \epsilon_{33}$$

All velocities are equal, and there is a "shear degeneracy" for all propagation directions (the slowness and velocity curves reduce to a single circle). In the tetragonal, hexagonal, and trigonal symmetries:

$$\epsilon_{11} = \epsilon_{22} \neq \epsilon_{33}$$

Finally, in the orthorhombic sysem:

$$\epsilon_{11} \neq \epsilon_{22} \neq \epsilon_{33}$$

Comparing the x- and y-propagating waves, we note that the z-polarized modes have the same velocity ($1/\sqrt{\mu\epsilon_{33}}$), but for the orthorhombic classes the velocity of the second mode depends on the propagation direction.

Recall that, in the acoustic case, for cubic symmetry in the principal planes there was a velocity-independent mode (the pure shear mode) and a second mode (the quasishear mode) in which the functional relationship between velocity and propagation direction was quite difficult to express in closed form. In the electromagnetic case, the form of the propagation-direction-dependent mode is simply an ellipse in all principal planes. We can derive expressions for the velocity in closed form by returning to (7.11). We require that the determinant of the coefficient matrix vanish. Thus,

$$\left(\frac{\omega^2}{k^2}\mu\epsilon_{11} - l_y^2\right)\left(\frac{\omega^2}{k^2}\mu\epsilon_{22} - l_x^2\right)\left(\frac{\omega^2}{k^2}\mu\epsilon_{33} - (l_x^2 + l_y^2)\right) - \left(\frac{\omega^2}{k^2}\mu\epsilon_{33} - (l_x^2 + l_y^2)\right)(l_x l_y)^2$$
$$= \left(\frac{\omega^2}{k^2}\mu\epsilon_{33} - (l_x^2 + l_y^2)\right)\left[\left(\frac{\omega^2}{k^2}\mu\epsilon_{11} - l_y^2\right)\left(\frac{\omega^2}{k^2}\mu\epsilon_{22} - l_x^2\right) - l_x^2 l_y^2\right] = 0 \tag{7.13}$$

(7.13) is the product of two terms that must be zero independently. The first term is the equation of a circle:

$$l_x^2 + l_y^2 = \frac{\omega^2}{k^2}\mu\epsilon_{33} \rightarrow \text{a circle of radius } \frac{\omega}{k}\sqrt{\mu\epsilon_{33}}$$

because $l_x^2 + l_y^2 = 1$. The phase velocity is simply,

$$v_p = \frac{\omega}{k} = \frac{1}{\sqrt{\mu\epsilon_{33}}} \tag{7.14}$$

and is independent of direction. This mode is called the *ordinary* mode. It is polarized in the z direction (and thus depends on ϵ_{33}) for all l_x and l_y, and thus (in acoustics terminology) a pure shear mode. In the xz plane, the formulation is identical except that $\epsilon_{33} \rightarrow \epsilon_{22}$ and the polarization of the ordinary mode is in the y direction. Similarly, in the yz plane the ordinary mode is x-polarized (see Figure 7.1). For the second term in (7.13), we write

$$l_x^2 l_y^2 - \left[\left(\frac{\omega^2}{k^2}\mu\epsilon_{11}\right)\left(\frac{\omega^2}{k^2}\mu\epsilon_{22}\right) + l_x^2 l_y^2 - l_y^2\frac{\omega^2}{k^2}\mu\epsilon_{22} - l_x^2\frac{\omega^2}{k^2}\mu\epsilon_{11}\right]$$
$$= l_y^2\frac{\omega^2}{k^2}\mu\epsilon_{22} + l_x^2\frac{\omega^2}{k^2}\mu\epsilon_{11} - \left(\frac{\omega^2}{k^2}\mu\epsilon_{11}\right)\left(\frac{\omega^2}{k^2}\mu\epsilon_{22}\right) = 0 \tag{7.15}$$

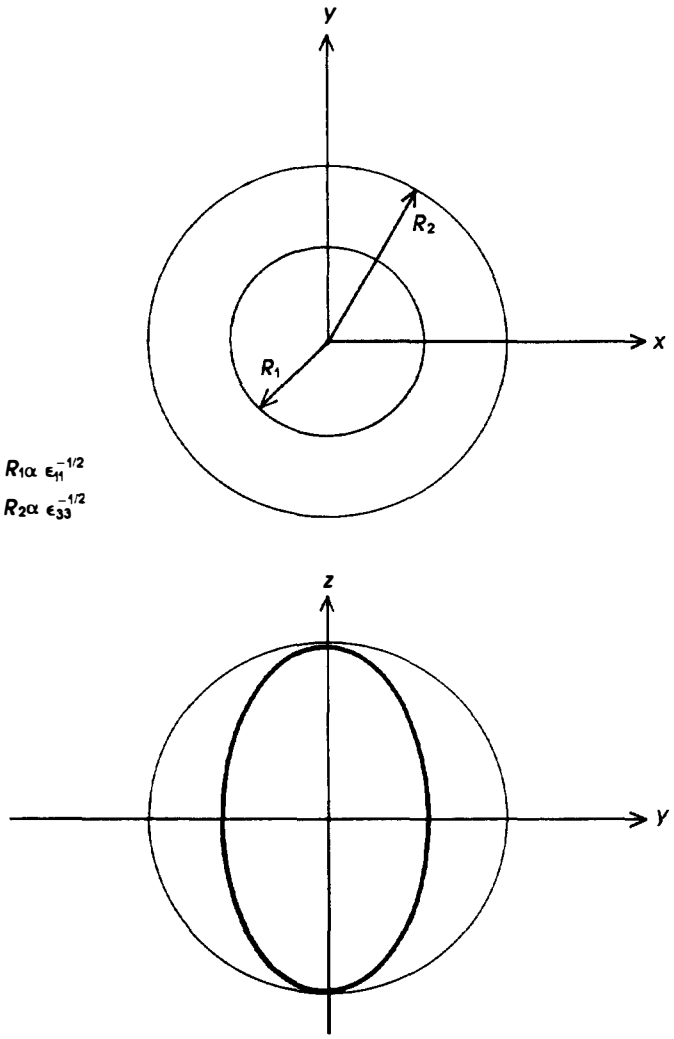

Figure 7.1 Optic velocity curves for uniaxial crystal: (a) xy plane, R_1 is proportional to $\epsilon_{11}^{-1/2}$ and R_2 is proportional to $\epsilon_{33}^{-1/2}$, (b) yz plane, the z-axis is the optic axis.

Equation (7.15) has the form:

$$\frac{l_x^2}{a^2} + \frac{l_y^2}{b^2} = 1 \tag{7.16}$$

where

$$a^2 = \frac{\omega^2}{k^2}\mu\epsilon_{22} \quad \text{and} \quad b^2 = \frac{\omega^2}{k^2}\mu\epsilon_{11}$$

This mode, in which the velocity depends on the propagation direction, is called the *extraordinary* mode. Like the slow shear mode for cubic symmetry in the principal planes, this mode is a quasishear mode and thus has a velocity component in the direction of propagation. It is a pure shear mode only for propagation along the principal axes (unlike the acoustic quasishear mode in cubic symmetry, which is also a pure mode at 45° to the principal axes). The form of (7.16) is elliptic, which is similar to that of the phase velocity of the pure shear mode in the orthorhombic symmetry in the principal planes (or the tetragonal symmetry in the yz or xz planes). If the permittivity contains off-diagonal terms (monoclinic and triclinic), then (7.16) is modified to a rotated ellipse similar to the case of the pure shear mode in the yz plane for trigonal symmetry.

Note that if $\epsilon_{11} = \epsilon_{22}$, then the ellipse degenerates into a circle of radius $(k/\omega)(1/\sqrt{\mu\epsilon_{11}})$ in the x-y plane. The slowness curves in this case consist of two concentric circles. When the three permittivity components are equal (isotropic and cubic symmetries), the two circles have identical radii and there is only one slowness curve, analogous to a shear degeneracy for all propagation directions (which occurs in the acoustic case only for isotropic symmetry).

In the xz plane, the phase velocity dependence for the extraordinary mode has the form:

$$\frac{l_x^2}{a^2} + \frac{l_z^2}{b^2} = 1 \tag{7.17}$$

where

$$a^2 = \frac{\omega^2}{k^2}\mu\epsilon_{33}, \quad b^2 = \frac{\omega^2}{k^2}\mu\epsilon_{11}$$

Again, in the cubic and isotropic symmetries, the velocities are equal for all propagation directions. For the hexagonal, trigonal, and tetragonal symmetries, however, the slowness curves consist of a circle and an ellipse. For a z-propagating wave in these symmetries, the velocity of the extraordinary mode is

$$v_p = \frac{1}{\sqrt{\mu\epsilon_{11}}}$$

which is identical to the ordinary mode velocity (because $\epsilon_{11} = \epsilon_{22}$). This direction, in which the velocities of the two modes are equal (a shear degeneracy), is called the *optic* axis. Symmetries with one optic axis (hexagonal, trigonal, and tetragonal) are called *uniaxial.* If all permittivity components are different (orthorhombic, monoclinic, and triclinic symmetries), the extraordinary mode is an ellipse in all planes. It can intersect the ordinary mode in two axes (or not at all). If the velocities of the two modes do cross, the axes of intersection (the propagation directions $\hat{\mathbf{l}}$) are the optic axes. Because there can be either two or no intersections, these crystals are called *biaxial.* These results are summarized in Table 7.2.

Table 7.2

Symmetry	*xy Plane*	*xz Plane*	*yz Plane*
Isotropic Cubic	One circle in all planes		
Hexagonal Trigonal Tetragonal	Two concentric circles	One circle, one ellipse, intersect at z-axis	One circle, one ellipse, intersect at z-axis
Orthorhombic	One ellipse and one circle in all planes two intersections, neither of which is the z-axis		

Recall that for acoustic modes, the particle velocity and displacement vectors are parallel because $\boldsymbol{v} = \dot{\mathbf{u}}$. For optic modes, the polarization is defined as the direction of the electric field, because **D** and **E** are *not* parallel. To determine the relationships between the electrical variable and $\hat{\mathbf{l}}$, we write Ampere's law in differential form:

$$\nabla \times \mathbf{H} = -\frac{\partial \mathbf{D}}{\partial t} \quad \text{or} \quad \hat{\mathbf{l}} \times \mathbf{H} = -\frac{\partial \mathbf{D}}{\partial t} \tag{7.18}$$

Equation (7.18) states that the propagation vector (in the direction of energy propagation) $\hat{\mathbf{l}}$ is normal to the displacement **D.**

Now consider the Poynting vector:

$$\mathbf{P} = \mathbf{E} \times \mathbf{H} \tag{7.19}$$

Equation (7.19) implies that the ray vector is normal to both **E** and **H**. That $\hat{\mathbf{l}}$ is normal to **B** can be seen from (7.1). Because **B** is parallel to **H** (μ is a scalar), $\hat{\mathbf{l}}$ is normal to **H**. Thus **E**, **D**, **P**, and $\hat{\mathbf{l}}$ are normal to **H** (and **B**) and are thus coplanar. We have already shown that **E** is not necessarily normal to $\hat{\mathbf{l}}$ (for the quasimode). Because **P** is always normal to **E** (from (7.19)), it is not generally normal to **D** (because **D** is not parallel to **E**). These facts are summarized in Figure 7.2. Note that the angle α depends on the propagation direction and is always zero for the ordinary mode. In acoustics terminology, we say that the power flow angle for the extraordinary mode depends on $\hat{\mathbf{l}}$, but for the ordinary mode the power flow angle is identically zero. Table 7.3 summarizes the properties of optic and acoustic modes.

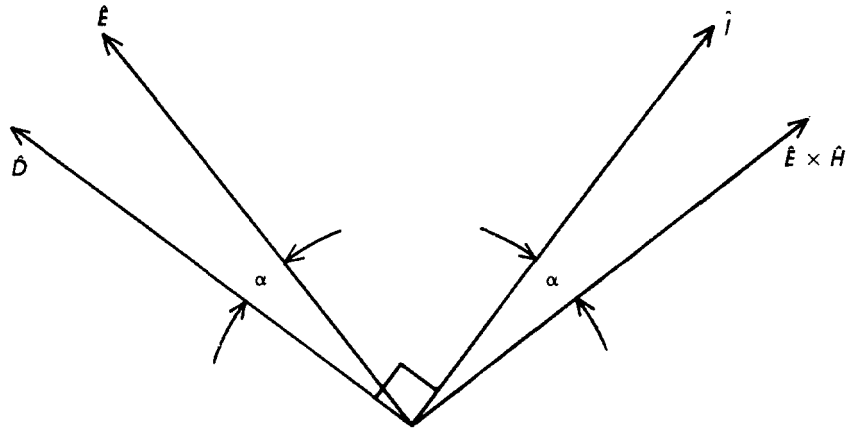

Figure 7.2 Relation of the electromagnetic fields in an anisotropic crystal. The angle α depends on the degree of birefringence (anisotropy), but is usually only a few degrees.

Table 7.3 Comparison of Optic and Acoustic Modes

Acoustic Modes	*Optic Modes*
Polarization is defined as direction of particle displacement	Polarization is defined as direction of electric field
Three orthogonal polarizations	Two orthogonal polarizations
Generally difficult to express velocities in closed form	Closed-form expressions (circles and ellipses)

Modes are generally neither parallel nor normal to $\hat{\mathbf{l}}$ (all modes quasi)	Both modes are shear; one is pure, the other quasi
Directions exist for which beam is self-collimating	No self-collimating directions exist

7.3 COMPUTER-AIDED SOLUTION OF OPTICAL MODES

The optical propagation matrix (7.10) is easily adaptable to computer solution for the velocities, inverse velocities (slowness), and polarizations of the permitted modes. For each propagation direction, there are *two* modes: one a pure shear, the other a quasishear. The form of the program is identical to the acoustic case. For a nonmagnetic crystal of symmetry up to and including the orthorhombic classes, the data consist of three numbers (the three permittivities along the principal axes). We write the 3×3 "Christoffel" matrix directly following the form of (7.10) without the more sophisticated analysis required in the acoustic case. The remaining part of the program is identical to the acoustic case; the roots of the characteristic equation are the velocities of the eigenmodes.

For a given $\hat{\mathbf{l}}$, there is always one pure mode (called the ordinary mode). The deviation angle of the quasi (extraordinary) mode is determined exactly as in the acoustic case. Like acoustic propagation, the polarization of the extraordinary mode is in a plane with normal parallel to the ordinary polarization. At 45° from a principal axis, the deviation is maximum. This behavior is similar to the deviation of the acoustic *pure* mode in tetragonal symmetry in the *yz* plane (for which the slowness also has an elliptic shape) and unlike the deviation of the quasishear mode in cubic symmetry, which is zero at 45°. The deviation angle for the extraordinary mode is, however, quite small compared with acoustic angles, being rarely greater than 3° except for extremely anisotropic crystals. For example, in the *yz* plane the maximum deviation of the extraordinary mode for $LiNbO_3$ (which is relatively anisotropic) is about 1.5° at .633 μm. Because the permittivity components vary with wavelength, the deviation angle also depends on wavelength.

Power flow angle and ray surface curves are determined in precisely the same manner as in the acoustic case. Again, because of the small optic anisotropies, power flow angles are generally quite small compared with the quasishear acoustic mode. Similarly, to a resonable approximation the

ray surface curves resemble circles. Because the shape of the extraordinary mode slowness curve is only slightly elliptic, the value of b (from (3.16)) is generally very close to zero; hence, there are no collimating directions, and focusing relies entirely on the presence of controlled inhomogeneities (i.e., variations of the permittivity with position).

7.4 THE INDEX ELLIPSOID

For propagation in isotropic or cubic crystals, there is only one (pure) shear mode; in all other classes, there are two propagating shear modes: one pure (called the ordinary mode), and one quasi (called the extraordinary mode). Thus, although the crystal properties require a maximum of six numbers (the components of the permittivity matrix), the propagation is described by two numbers (the roots of the characteristic equation). This behavior is qualitatively similar to the acoustic case in which the crystal is described by a maximum of 21 numbers, but the propagation characteristics are described by 3. Because of the relatively simple form of (7.10) (compared with the acoustic propagation), it is possible to derive an alternative formulation of the propagation of electromagnetic waves in anisotropic media. The formulation involves only one surface, called the *index ellipsoid,* which encompasses all the necessary information of the two optical modes. It involves the orthogonal triad $\mathbf{D}_1$, $\mathbf{D}_2$, and $\hat{\mathbf{l}}$ (7.18), where $\mathbf{D}_1$ and $\mathbf{D}_2$ are displacement vectors of the propagating modes. The index ellipsoid has no analogue for bulk acoustic modes.

To form the index ellipsoid, consider the electric energy density in an electromagnetic wave with symmetry up to orthorhombic (only three independent components of $\mathbf{U}$):

$$\begin{aligned} u_E &= \frac{1}{8\pi}\,\mathbf{E}\cdot\mathbf{D} \\ &= \frac{1}{8\pi}\left(\epsilon_{11}E_x^2 + \epsilon_{22}E_y^2 + \epsilon_{33}E_z^2\right) \\ &= \frac{1}{8\pi}\left(\frac{D_x^2}{\epsilon_{11}} + \frac{D_y^2}{\epsilon_{22}} + \frac{D_z^2}{\epsilon_{33}}\right) \end{aligned} \tag{7.20}$$

If we let

$$n_1 = \sqrt{\epsilon_{11}}, \quad n_2 = \sqrt{\epsilon_{22}}, \quad n_3 = \sqrt{\epsilon_{33}}$$

where the values of n are the indices of refraction along the principal axes, (7.20) becomes

$$u_E = \frac{1}{8\pi}\left(\frac{D_x^2}{n_1^2} + \frac{D_y^2}{n_2^2} + \frac{D_z^2}{n_3^2}\right) \tag{7.21}$$

We now make the substitutions:

$$x = \frac{D_x}{8\pi}, u_E \quad y = \frac{D_y}{8\pi}, u_E \quad z = \frac{D_z}{8\pi} u_E$$

and (7.21) becomes

$$1 = \frac{x^2}{n_1^2} + \frac{y^2}{n_2^2} + \frac{z^2}{n_3^2} \tag{7.22}$$

Equation (7.22) is the equation of an ellipsoid (in three-dimensional space) and is called the *index ellipsoid* or, simply, *indicatrix*. In the present case (diagonal permittivity), the axes of the indicatrix are located along the principal coordinate axes; if the permittivity possesses off-diagonal terms, the indicatrix would be rotated in the Cartesian system. Note that the n values are scalars, and the ϵ values are components of the permittivity matrix. If the crystal is uniaxial, $\epsilon_{11} = \epsilon_{22}$ for hexagonal, trigonal, and tetragonal symmetries and the indicatrix becomes an ellipsoid of revolution (about the optic or z-axis) for these classes. Formally, we write

$$1 = \frac{x^2}{n_o^2} + \frac{y^2}{n_o^2} + \frac{z^2}{n_e^2} \tag{7.23}$$

where

$$n_o = \sqrt{\epsilon_{11}} = \sqrt{\epsilon_{22}} \quad \text{and} \quad n_e = \sqrt{\epsilon_{33}}$$

n_o is called the ordinary index of refraction, and n_e is the extraordinary index. The ordinary and extraordinary polarizations can also be constructed from the index ellipsoid [1].

To understand (7.23), let the propagation vector $\hat{\mathbf{l}}$ lie in the yz plane. There are two modes and thus two **D** vectors that are normal to $\hat{\mathbf{l}}$. The two roots are simply the intersections of these vectors with the indicatrix. One of the intersections is along the x-axis and has the phase velocity c/n_0, where c is the velocity in vacuum. This is the ordinary mode. The other intersection (which depends on $\hat{\mathbf{l}}$) is shown in Figure 7.3 and is

$$\frac{\cos^2(\theta)}{n_o^2} + \frac{\sin^2(\theta)}{n_e^2} = \frac{1}{n_e^2(\theta)} \tag{7.24}$$

where θ is measured from the optic axis. At $\theta = 0$, $n_e(\theta) = n_o$ as expected. We should be careful not to confuse $n_e(\theta)$ (which is a root of the characteristic equation) with n_e, just as we should not confuse the roots of the Christoffel equation with the individual stiffness components. The phase velocity of the extraordinary mode is $c/n_e(\theta)$.

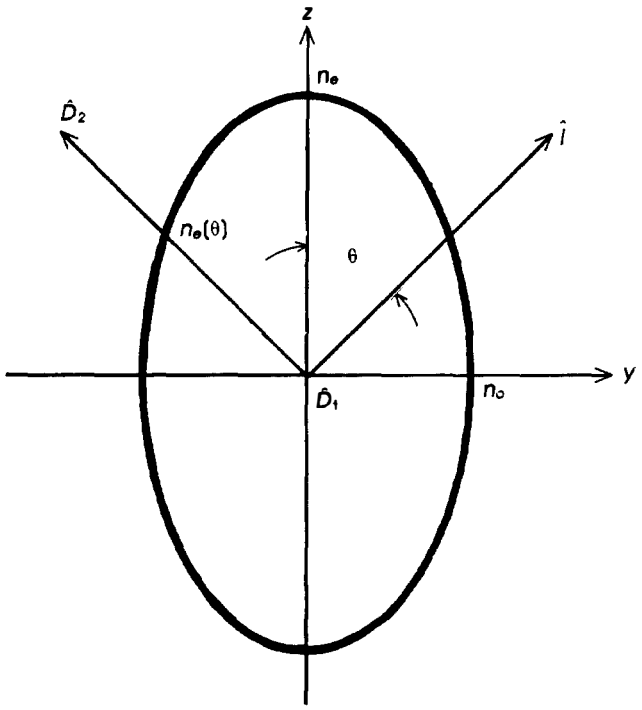

Figure 7.3 The index ellipsoid in the yz plane for a uniaxial crystal. For a propagation direction $\hat{\mathbf{l}}$ along the z (optic) axis $n_e(\theta) = n_o$ and $\mathbf{D}_2$ is oriented along y.

An alternative form of (7.22) is

$$B_{11}x^2 + B_{22}y^2 + B_{33}z^2 = 1 \tag{7.25}$$

where B_{11}, B_{22}, and B_{33} are components of the *impermeability matrix* and

$$B_{11} = n_1^{-2},\ B_{22} = n_2^{-2},\ B_{33} = n_3^{-3}$$

Written in form of (7.25), the impermeability matrix **B** can possess off-diagonal terms. The off-diagonal terms have so far not been required in the description of the propagation characteristics (because we deal with systems up to orthorhombic), but such terms can appear even in the isotropic system if the index ellipsoid is perturbed by the presence of electrical or mechanical fields. The only requirement here is that **B** be symmetric (i.e., possess six independent terms). Equation (7.25) is modified to account for these terms; we write

$$B_{11}x^2 + B_{22}y^2 + B_{33}z^2 + 2B_{12}xy + 2B_{13}xz + 2B_{23}yz = 1$$

or, in summation notation,

$$B_{ij}x_ix_j = 1 \qquad i = 1 \text{ to } 3, \quad j = 1 \text{ to } 3 \tag{7.26}$$

where $x_i = x$, $x_2 = y$, and $x_3 = z$.

In (7.26), the components of **B** are written in the single subscript notation as

$$B_{11} = B_1, \quad B_{22} = B_2, \quad B_{33} = B_3$$

$$B_{12} = B_6, \quad B_{13} = B_5, \quad B_{23} = B_4$$

Formally, (7.26) can be written as

$$\tilde{\mathbf{r}}:\mathbf{B}:\mathbf{r} = 1$$

7.5 PERTURBATIONS TO THE INDEX ELLIPSOID

An electric field or a mechanical stress causes the indices of refraction to change. We describe the *perturbed* index ellipsoid by breaking the impermeability matrix into two components; for the unperturbed index, we write

$$B^0_{ij}x_ix_j = 1 \qquad \text{(unperturbed state)} \tag{7.27}$$

where B^0_{ij} are the unperturbed impermeability components. Usually $\mathbf{B}^0$ will not have off-diagonal terms if we consider symmetry classes up to orthorhombic.

If an electrical or mechanical field is applied, there is a perturbation term that generally will involve all six impermeability components:

$$B_{ij} \rightarrow B_{ij}^0 + \Delta B_{ij} \tag{7.28}$$

where

$$\Delta B_{ij} = r_{ijk}E_k + \pi_{ijkl}T_{kl} \tag{7.29}$$

The r_{ijk} are called the electro-optic coefficients, and the π_{ijkl} are the piezo-optic coefficients. The perturbation also changes the optic slowness curves in much the same way that piezoelectricity changed the acoustic slowness curves. Indeed, we can think of the optic slowness curves as being "electro-optically" or "piezo-optically" stiffened (the stiffening can be positive or negative). It is more convenient, however, to use the index ellipsoid formalism than the two optic slowness curves.

We now examine each of the terms in (7.29) separately. The electro-optic coefficients couple a 3×1 vector (**E**) to a 3×3 matrix **B**; this coupling requires 3^3 components. This situation is identical to the one we encountered in our discussion of piezoelectricity, in which an electric field (3×1 vector) couples to a stress or strain matrix. Because the perturbed impermeability matrix, like the stress or strain matrices, is symmetric, there must be interchange symmetry between i and j:

$$r_{ijk} \rightarrow r_{Ik} \qquad I = 1 \text{ to } 6$$

We can therefore write the electro-optic coefficients in the form of a 6×3 matrix with, in general, 18 independent components; the precise number of independent components is determined by the symmetry class. As in piezoelectricity the electro-optic matrix vanishes for those symmetry classes that possess inversion symmetry. Indeed, for all classes the form of the electro-optic and piezoelectric matrices are identical because both are derived from the fundamental symmetry operations of each symmetry class (Neumann's principle).

Example 7.1. Electro-Optic Effect in GaAs. The form of the electro-optic matrix is (compare this form with the piezoelectric matrix for GaAs)

$$r_{Ik} = \begin{bmatrix} 0 & 0 & 0 \\ 0 & 0 & 0 \\ 0 & 0 & 0 \\ r_{41} & 0 & 0 \\ 0 & r_{41} & 0 \\ 0 & 0 & r_{41} \end{bmatrix} \tag{7.30}$$

The unperturbed indicatrix for GaAs is simply a sphere (cubic symmetry):

$$\frac{1}{n_o^2}(x^2 + y^2 + z^2) = 1 \tag{7.31}$$

The perturbation due to an electric field is

$$\Delta B_{ij} = r_{ijk}E_k \text{ or } \Delta B_I = r_{Ik}E_k \tag{7.32}$$

The impermeability components (such as permittivity) are dimensionless, so the units of electro-optic components are the inverse of the electric field units, or *m*/V. If we assume that the electric field is *z*-directed, we have (from (7.23) and (7.30))

$$\Delta B_I = r_{Ik}E_k$$

$$\Delta B_I = \begin{bmatrix} 0 & 0 & 0 \\ 0 & 0 & 0 \\ 0 & 0 & 0 \\ r_{41} & 0 & 0 \\ 0 & r_{41} & 0 \\ 0 & 0 & r_{41} \end{bmatrix} \begin{bmatrix} 0 \\ 0 \\ E_z \end{bmatrix} = \begin{bmatrix} 0 \\ 0 \\ 0 \\ 0 \\ 0 \\ r_{41}E_z \end{bmatrix} = \begin{bmatrix} 0 \\ 0 \\ 0 \\ 0 \\ 0 \\ \Delta B_6 \end{bmatrix} \tag{7.33}$$

The form of (7.33) would be similar had we applied an *x*- or *y*-directed field (for E_x we would have ΔB_4 and for E_y, ΔB_5). Alternatively, we write ΔB as

$$\Delta B_{ij} = \begin{bmatrix} 0 & \frac{r_{41}E_z}{2} & 0 \\ \frac{r_{41}E_z}{2} & 0 & 0 \\ 0 & 0 & 0 \end{bmatrix} \tag{7.34}$$

Because the perturbation involves $B_6 = B_{12}$, the perturbed indicatrix is written as

$$\underset{\substack{\uparrow \\ \text{unperturbed component}}}{\frac{1}{n_o^2}(x^2 + y^2 + z^2)} + \underset{\substack{\uparrow \\ \text{perturbation}}}{r_{41}E_z\, xy} = 1 \tag{7.35}$$

The form of (7.35) is no longer a sphere. By introducing a cross term in the index ellipsoid, the electric field has created a *birefringence* (anisotropy)

in an optically isotropic crystal; the magnitude of the anisotropy depends on the matrix component r_{41} and the strength of the electric field. We will return to this example later.

Example 7.2: Electro-Optic Effect in $LiNbO_3$. The form of the electro-optic matrix is (compare this form with the piezoelectric matrix for $LiNbO_3$)

$$r_{Ij} = \begin{bmatrix} 0 & -r_{22} & r_{13} \\ 0 & r_{22} & r_{13} \\ 0 & 0 & r_{33} \\ 0 & r_{51} & 0 \\ r_{51} & 0 & 0 \\ -r_{22} & 0 & 0 \end{bmatrix} \tag{7.36}$$

Because $LiNbO_3$ is trigonal, the unperturbed indicatrix is an ellipsoid of revolution about the z- (optic) axis:

$$\frac{x^2}{n_o^2} + \frac{y^2}{n_o^2} + \frac{z^2}{n_e^2} = 1 \tag{7.37}$$

From (7.29), the presence of an electric field causes a perturbation in the impermeability matrix:

$$\Delta B_{ij} = r_{Ik}E_K = \Delta B_I \qquad I = 1 \text{ to } 6 \tag{7.38}$$

As in Example 7.1, we apply the electric field in the z direction.

$$\mathbf{E} = E_z\,\hat{\mathbf{i}}$$

Then, from (7.36) the perturbation becomes

$$\Delta B_I = \begin{bmatrix} r_{13}E_z \\ r_{13}E_z \\ r_{33}E_z \\ 0 \\ 0 \\ 0 \end{bmatrix} \tag{7.39}$$

The perturbed index ellipsoid is

$$x^2\left(\frac{1}{n_o^2} + r_{13}E_z\right) + y^2\left(\frac{1}{n_o^2} + r_{13}E_z\right) + z^2\left(\frac{1}{n_e^2} + r_{33}E_z\right) = 1 \tag{7.40}$$

In this case, the form of the birefringence has not changed (the crystal remains uniaxial and there are no cross terms), but the magnitude of the indices now depends on the electric field. If the perturbations are small compared with the unperturbed indices, the new indices are written as

$$n_o \rightarrow \frac{n_o}{(1 - r_{13}E_z n_o^2)^{-1/2}} \sim n_o\left(1 - \frac{r_{13}E_z}{2} n_o^2\right) \tag{7.41}$$

and

$$n_e \rightarrow n_e\left(1 - \frac{r_{13}E_z}{2} n_e^2\right)$$

7.6 THE PIEZO-OPTIC EFFECT

A stress changes the index ellipsoid in much the same way that an electric field does. Unlike the electro-optic effect, the piezo-optic or photoelastic effect exists for all symmetry classes because it results from a coupling between two 3 × 3 matrices (water, for example, possesses a particularly strong piezo-optic effect). From (7.29), we write

$$\Delta B_{ij} = \pi_{ijkl} T_{kl} \tag{7.42}$$

Because ΔB_{ij} and T_{kl} are symmetric, (7.42) simplifies to

$$\Delta B_I = \pi_{IK} T_K, \quad I = 1 \text{ to } 6, \; K = 1 \text{ to } 6 \tag{7.43}$$

where π_{IK} is called the piezo-optic matrix.

The piezo-optic matrix is identical to the form of the stiffness matrix, which also couples two 3 × 3 symmetric matrices. For stiffness (and compliance) matrices, however, we showed from energy consideration that

$$c_{IK} = c_{KI} \quad \text{and} \quad s_{IK} = s_{KI}$$

This symmetry condition reduced the maximum number of independent components from 36 to 21. Unfortunately, no such condition exists for the piezo-optic matrix. As always, the symmetry of a particular class determines the precise form of the piezo-optic matrix, but in general its form will be somewhat more complex than that of the stiffness matrix. For example, the piezo-optic matrix in the triclinic system possesses the full 36 possible independent components, and the monoclinic has 20. Although

not of direct interest, we note that a quadratic electro-optic effect exists, in which $\Delta\mathbf{B}$ is proportional to the *product* of electric fields. This effect, like the piezo-optic effect, exists for all symmetries. The coupling matrix requires 3^4 components and thus has the same symmetry as the piezo-optic and stiffness matrices.

Because the piezo-optic matrix couples the impermeability to stress, it is usually used for static situations. When dealing with acoustic waves, we will find it more convenient to work with the strain matrix, because it is related to the particle displacement (acoustic polarization). This situation is analogous to the acoustic case, where we defined two related matrices: the piezoelectric strain matrix **d** (for static problems) and the piezoelectric stress matrix **e** (for acoustic waves). The choice of which is used in a particular problem depends on whether the stress or the strain is chosen as the independent variable. We write

$$\Delta B_{ij} = p_{ijrs} S_{rs} = \pi_{ijkl} T_{kl} \tag{7.44}$$

The components of the impermeability matrix are dimensionless. Hence the units of the piezo-optic matrix π are m^2/N (the inverse of **T**). From Hooke's law,

$$T_{kl} = c_{klrs} S_{rs}$$

Substituting this relation into (7.44), we get

$$\Delta B_{ij} = \pi_{ijkl} c_{klrs} S_{rs} = p_{ijrs} S_{rs} \tag{7.45}$$

From (7.44),

$$p_{ijrs} = \pi_{ijkl} c_{klrs}$$

or

$$p_{IR} = \pi_{IK} c_{KR} \qquad I, K, \text{and } R = 1 \text{ to } 6 \tag{7.46}$$

where p_{IR} is called the *photoelastic* or *strain-optic* matrix, similar to the piezo-optic matrix: $p_{IR} \neq p_{RI}$. Because the components of the impermeability **B** and strain **S** matrices components are dimensionless, the components of the photoelastic matrix are also dimensionless.

Example 7.3: Piezo-Optic Effect in a Cubic Crystal We calculate the change in the indicatrix due to the application of a static stress in GaAs (class $43m$). The form of the piezo-optic matrix is derived by using Neumann's principle and is

$$\boldsymbol{\Pi} = \begin{bmatrix} \pi_{11} & \pi_{12} & \pi_{12} & 0 & 0 & 0 \\ \pi_{12} & \pi_{11} & \pi_{12} & 0 & 0 & 0 \\ \pi_{12} & \pi_{12} & \pi_{11} & 0 & 0 & 0 \\ 0 & 0 & 0 & \pi_{44} & 0 & 0 \\ 0 & 0 & 0 & 0 & \pi_{44} & 0 \\ 0 & 0 & 0 & 0 & 0 & \pi_{44} \end{bmatrix} \tag{7.47}$$

Note that for this particular case, the matrix is symmetric and there are three independent constants (this is due entirely to the symmetry of the $\bar{4}3m$ class). We apply a longitudinal stress in the z direction:

$$T_{ij} = T_{33} = T_3$$

The unperturbed indicatrix is given by (7.31) (a sphere). The perturbation is given by (7.44):

$$\Delta B_{ij} = \Delta B_I = \pi_{IK} T_K$$

with $T_K = T_3$ and

$$\begin{bmatrix} \Delta B_1 \\ \Delta B_2 \\ \Delta B_3 \\ \Delta B_4 \\ \Delta B_5 \\ \Delta B_6 \end{bmatrix} = \begin{bmatrix} \pi_{11} & \pi_{12} & \pi_{12} & 0 & 0 & 0 \\ \pi_{12} & \pi_{11} & \pi_{12} & 0 & 0 & 0 \\ \pi_{12} & \pi_{12} & \pi_{11} & 0 & 0 & 0 \\ 0 & 0 & 0 & \pi_{44} & 0 & 0 \\ 0 & 0 & 0 & 0 & \pi_{44} & 0 \\ 0 & 0 & 0 & 0 & 0 & \pi_{44} \end{bmatrix} \begin{bmatrix} 0 \\ 0 \\ T_3 \\ 0 \\ 0 \\ 0 \end{bmatrix} \tag{7.48}$$

Performing the matrix multiplication, we find

$$\Delta B_1 = \pi_{12} T_3, \quad \Delta B_2 = \pi_{12} T_3, \quad \Delta B_3 = \pi_{11} T_3$$

The perturbed index ellipsoid is

$$x^2\left(\frac{1}{n_o^2} + \pi_{12} T_3\right) + y^2\left(\frac{1}{n_o^2} + \pi_{12} T_3\right) + z^2\left(\frac{1}{n_o^2} + \pi_{11} T_3\right) = 1 \tag{7.49}$$

In general, $\pi_{11} \neq \pi_{12}$, so (7.49) is the equation of an ellipsoid of revolution about the z-axis. The effect of z-directed stress is to create a birefringence in the crystal proportional to the magnitude of the applied stress, thus transforming the cubic GaAs into a uniaxial medium. Note the similarity between (7.49) and (7.40) (z-directed electric field in lithium niobate). If the perturbation is small, the new indices are

$$n_o' = n_o - \tfrac{1}{2}n_o^3\pi_{12}T_3 \quad \text{(for the } x\text{- and } y\text{-axes)}$$

$$n_e' = n_o - \tfrac{1}{2}n_o^3\pi_{11}T_3 \quad \text{(for the } z\text{-axis)} \tag{7.50}$$

where n_o is the unperturbed index of refraction.

For the cubic classes 23 and $m3$, $\pi_{12} \neq \pi_{13}$ and the application of a stress T_3 would have resulted in a biaxial anisotropy. Examples of such materials are bismuth germanium oxide, bismuth silicon oxide, and hydrogen sulfide. For GaAs, the birefringence is (defined as the difference between the ordinary and extraordinary indices)

$$n_o' - n_e' = \tfrac{1}{2}n_o^3(\pi_{11} - \pi_{12})T_3 \tag{7.51}$$

As in Examples 7.1 and 7.2, the magnitude of the anisotropy depends on the strength of the stress T_3. To get a quantitative feel for the anisotropy, we substitute values into (7.51). It is usually easier to find the components of the photoelastic matrix in tabulated form, so we convert the π components to p components, using (7.46):

$$\mathbf{p} = \mathbf{\Pi}\mathbf{:c} \tag{7.52}$$

Multiplying on the right by the compliance **s** gives

$$\mathbf{p:s} = \mathbf{\Pi:c:s} \tag{7.53}$$

but

$$\mathbf{c:s} = \mathbf{s:c} = \mathbf{I}$$

so

$$\mathbf{\Pi} = \mathbf{p:s} \tag{7.54}$$

We need π_{11} and π_{12}; for GaAs (recall that photoelastic components are dimensionless);

$$p_{11} = -.165,\ p_{12} = -.14,\ p_{44} = -.072$$

$$s_{11} = 12.6 \times 10^{-12}\ \text{m}^2/\text{N},\ s_{12} = -4.23 \times 10^{-12}\ \text{m}^2/\text{N},$$

$$s_{44} = 18.6 \times 10^{-12}\ \text{m}^2/\text{N}$$

From (7.54);

$$\pi_{11} = \sum_{1}^{6} p_{1r}s_{r1} = p_{11}s_{11} + p_{12}s_{21} + p_{13}s_{31} \sim -9.2 \times 10^{-12}\ \mathrm{m^2/N}$$

Similarly,

$$\pi_{12} \sim .7 \times 10^{-12}\ \mathrm{m^2/N}$$

Note the difference in magnitudes between the piezo-optic and photoelastic components. The unperturbed refractive index of GaAs at 1.06 μm (Nd:YAG laser) is approximately 3.4, and thus the birefringence is (from (7.51))

$$n_o' - n_e' = \tfrac{1}{2}n_o(\pi_{12} - \pi_{11}) \sim -3.2 \times 10^{-11}T_3$$

A birefringence of 10^{-3} (a relatively small but potentially useful value) requires that

$$T_3 = 3.1 \times 10^7\ \mathrm{N/m^2} \text{ or } 4400\ \mathrm{psi}$$

For a typical device area A (5 mm × 5 mm cross section), the required force is therefore

$$F = T_3A = 78\ \mathrm{kg}$$

We conclude that it takes a relatively large static force to produce even a small birefringence.

7.7 POLARIZATION ROTATIONS

Next, we consider the case in which the perturbed index ellipsoid contains "cross terms." Returning to the example of the electro-optic effect in GaAs (the results are equally applicable to the piezo-optic effect), we rewrite (7.35):

$$\frac{x^2 + y^2 + z^2}{n_o^2} + r_{41}E_z xy = 1$$

Equation (7.35) has the form:

$$B_{ij}^0(x^2 + y^2 + z^2) + \Delta B_{ij}xy = 1 \tag{7.55}$$

where

$$B_{ij} = B_{ij}^0 + \Delta B_{ij}$$

is the symmetric matrix given by

$$\mathbf{B} = \begin{bmatrix} B^0 & \Delta B & 0 \\ \Delta B & B^0 & 0 \\ 0 & 0 & B^0 \end{bmatrix}$$

We need only consider the part of (7.55) that contains the "off-diagonal" terms:

$$[x\ y]\begin{bmatrix} B^0 & \Delta B \\ \Delta B & B^0 \end{bmatrix}\begin{bmatrix} x \\ y \end{bmatrix} = 1 \tag{7.56}$$

Equation (7.55) has the form of an ellipse that is *rotated* by 45° in the xy plane. As the perturbation decreases, the rotation angle does not change but the major and minor axes of the ellipse converge (it becomes more circular). Because the rotation angle is 45°, (7.55) is easy to diagonalize. Recall that a symmetric matrix transforms according to (1.81):

$$\mathbf{B}' = \tilde{\mathbf{R}}:\mathbf{B}:\mathbf{R}$$

where $\mathbf{R}$ is an orthogonal rotation matrix. Because $\mathbf{R}$ is orthogonal:

$$\mathbf{R}^{-1} = \tilde{\mathbf{R}}$$

In this example, we let $\mathbf{R}$ be the 45° rotation matrix about the z-axis:

$$\mathbf{R} = \frac{1}{\sqrt{2}}\begin{bmatrix} 1 & 1 \\ -1 & 1 \end{bmatrix}$$

Equation (1.81) becomes

$$\begin{aligned} \tilde{\mathbf{R}}:\mathbf{B}:\mathbf{R} &= \frac{1}{2}\begin{bmatrix} 1 & -1 \\ 1 & 1 \end{bmatrix}\begin{bmatrix} B^0 & \Delta B \\ \Delta B & B^0 \end{bmatrix}\begin{bmatrix} 1 & 1 \\ -1 & 1 \end{bmatrix} \\ &= \frac{1}{2}\begin{bmatrix} 1 & -1 \\ 1 & 1 \end{bmatrix}\begin{bmatrix} B^0 - \Delta B & B^0 + \Delta B \\ \Delta B - B^0 & \Delta B + B^0 \end{bmatrix} \end{aligned}$$

$$\tilde{\mathbf{R}}:\mathbf{B}:\mathbf{R} = \begin{bmatrix} B^0 & 0 \\ 0 & B^0 \end{bmatrix}$$

We apply the matrix $\mathbf{R}$ to the perturbed index ellipsoid:

$$\begin{bmatrix} x' \\ y' \end{bmatrix} = \mathbf{R}\begin{bmatrix} x \\ y \end{bmatrix} \text{ and } \begin{bmatrix} x \\ y \end{bmatrix} = \mathbf{R}^{-1}\begin{bmatrix} x' \\ y' \end{bmatrix} \tag{7.57}$$

Solving (7.57) for x and y in terms of x' and y' and substituting into (7.55), we obtain

$$\left(\frac{1}{n_o^2} + r_{41}E_z\right)x'^2 + \left(\frac{1}{n_o^2} - r_{41}E_z\right)y'^2 + \frac{z^2}{n_o^2} = 1 \tag{7.58}$$

The x'- and y'-axes are oriented at 45° with respect to the x- and y-axes, as shown in Figure 7.4. The form of the indicatrix is

$$\frac{x'^2}{n_x'^2} + \frac{y'^2}{n_y'^2} + \frac{z^2}{n_o^2} = 1 \tag{7.59}$$

where

$$n_x' = n_o - \frac{n_o^3}{2} r_{41}E_z \text{ and } n_y' = n_o + \frac{n_o^3}{2} r_{41}E_z$$

From the form of (7.59), we see that all the principal axes have different indices, and thus the field has transformed the optically isotropic GaAs into a biaxial crystal. Equation (7.59) defines the eigenmodes of the perturbed index ellipsoid as the principal axes of the perturbed ellipsoid. An optic wave propagating in the crystal and polarized along one of the principal axes, for example the x'-axis, will remain polarized along x'. A wave not polarized along with one of these axes undergoes a rotation in its polarization. To show this, we refer to Figure 7.4. We consider a z-propagating optic wave that at $z = 0$ is linearly polarized along the x-axis (which is *not* an eigenmode):

$$E_x = A\, e^{-j(\omega t - kz)} = A\, e^{-j(\omega t - n_o z/c)} \tag{7.60}$$

We decompose this field into the "eigenmodes" that lie along the principle directions x' and y':

$$E_{x'} = \frac{A}{\sqrt{2}} e^{-j(\omega t - n_{x'} z/c)}$$
$$E_{y'} = \frac{A}{\sqrt{2}} e^{-j(\omega t - n_{y'} z/c)} \tag{7.61}$$

which are valid at $z = 0$ and where $n_{x'}$ and $n_{y'}$ are given in (7.59). Clearly, at $z = 0$ the two waves are in phase and add to yield E_x. As they progress through the crystal, they move out of phase because their velocities are different ($n_{x'} \neq n_{y'}$). The y component (which was initially zero) grows at the expense of the x component. When the waves are π radians out of phase, the x component is zero. The corresponding position (z) is (from (7.59)

$$z' = \frac{c\pi}{\omega(n_x' - n_y')} \tag{7.62}$$

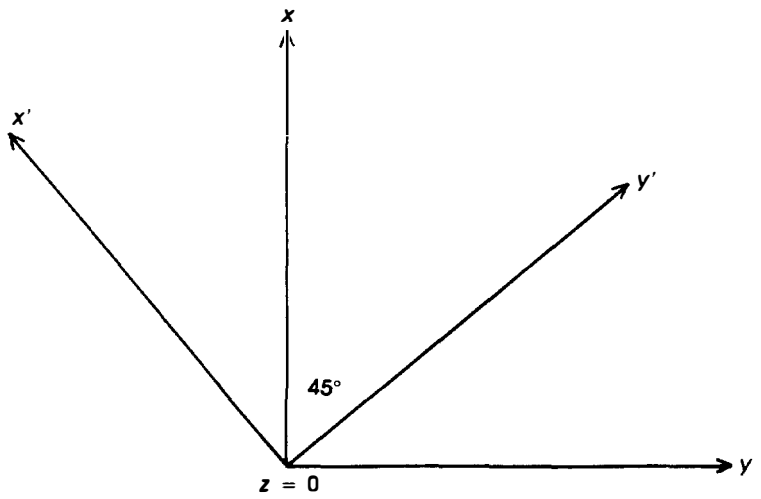

Figure 7.4 Relation of the rotated and unrotated coordinate systems for index ellipsoid with cross terms (see (7.58)). At $z = 0$, the electric field is oriented along x, whereas at $z = z'$ it rotates to y.

For a birefringence of 10^{-3}, a typical value of z' would be 1 mm. Whenever there is a cross term in the index ellipsoid, a propagating optic beam will always experience a polarization rotation. In acoustic wave propagation, the same phenomenon occurs when a wave propagates in a

direction in which there are two shear modes with different velocities, as we have already noted in Chapter 2. If the acoustic signal is a short pulse, because of the large fractional difference in velocity, it may spread significantly or even separate into two pulses. In optic propagation, pulse spreading occurs only over long distances, such as would be encountered in an optic fiber.

From the form of (7.26), it should be clear that cross terms require the presence of the perturbation terms ΔB_4, ΔB_5, or ΔB_6. In the electro-optic effect, the form of the **r** matrix and the direction of the electric field determine their presence. Each symmetry must be studied individually. In gallium arsenide, e.g., an arbitrarily directed electric field results in cross terms in the index ellipsoid, whereas in lithium niobate an x-directed field produces cross terms, but a z-directed field does not.

The form of the piezo-optic matrix is similar to the stiffness matrix (without the off-diagonal symmetry). For the isotropic, cubic, hexagonal, and orthorhombic classes, the general form is given in (7.48) (the relations between components depend on the particular class). In these classes, it is clear that only a shear stress will result in the presence of cross terms (through π_{44}, π_{55}, or π_{66}). In the tetragonal classes 4 and $4/m$, the form of the piezo-optic matrix is given by (2.99). The presence of the terms π_{51} and π_{61} couple longitudinal stresses T_1 and T_2 to ΔB_6. In the important class $4mm$, these terms are not present, and thus only shear stresses cause cross terms. The form of the piezo-optic matrix for trigonal classes ($3m$, 32, and $\bar{3}m$) is given by (4.56). In this symmetry, the presence of π_{41} and π_{42} couple the stresses T_1 and T_2 to the perturbation ΔB_4. We will investigate these coupling terms further in Chapter 9.

If the electric field varies with time, the index ellipsoid will likewise have a time-dependent component. In Example 7.2, the major axis of the ellipse will "vibrate" at the electric field frequency. In Example 7.1, the rotation of the optic polarization will vary at the external field frequency. This phenomenon can be used to modulate an optic wave. Modulators have been fabricated at frequencies up to 5 GHz by using this effect. Similar effects occur with mechanical stresses in which sinusoidal longitudinal stresses generally result in "pulsating" ellipsoids, and sinusoidal shear stresses result in a modulated optic beam.

Acousto-optics refers to the situation in which the perturbation to the index ellipsoid is due to the presence of an acoustic *wave*. In this case, it is convenient to use the strain as the independent variable (because strain is directly related to the acoustic polarization—i.e., the particle velocity). Thus, we prefer the photoelastic matrix over the piezo-optic matrix, although it is possible to use the piezo-optic matrix if the stress associated with the acoustic mode can be determined. The presence of a

strain wave causes a *spatially* periodic perturbation to the optic wave. Because the optic velocity is five orders greater than the acoustic velocity, the acoustic wave is stationary during the time it is traversed by the optic beam. The situation is analogous to the perturbation of an x-ray due to a periodic array of atoms. The perturbation of the index ellipsoid is described by the photoelastic matrix, which generally increases the birefringence of the medium. In this case, however, there is an additional effect that couples energy out of the incident beam and into a *diffracted* beam, with the strength of the perturbation determining the degree of energy extracted from the main beam. Cross terms in the perturbed index ellipsoid (caused by the wave) result in rotations as in the static case, with one important difference, which will be clarified later. The quantitative description of the coupling requires the theory of coupled mode theory.

7.8 COUPLED MODE THEORY OF ACOUSTO-OPTIC INTERACTION

The previous example showed how one particular mode grows at the expense of another. In general, an incident mode will be transformed in the crystal by the action of an electric field or an acoustic wave. Exiting the crystal are the incident and transformed beams, which may be deflected, frequency-shifted, or polarization-rotated, depending on the particular interaction. In this section, we consider the effect of the A/O interaction on an incident optic beam. Consider the usual unperturbed electromagnetic wave equation (4.35):

$$\nabla^2\mathbf{E} = \mu\epsilon\frac{\partial^2\mathbf{E}}{\partial t^2}, \quad \mu = \mu_0, \quad \epsilon = \epsilon_r\epsilon_0 = n^2\epsilon_0$$

Application of a strain changes the permittivity, as we have seen, so that

$$\epsilon' = \epsilon + \Delta\epsilon \tag{7.63}$$

where $\Delta\epsilon$ is the perturbed permittivity (the ΔB), which depends on the coupling of the perturbation with the photoelastic matrix. Equation (7.63) assumes that we have solved for the directional properties of the coupling. This situation is similar to the development of the Mason model, where we assume that the eigenmodes are known. Substituting (7.63) into (4.35) gives

$$\nabla^2\mathbf{E} = \mu\epsilon\frac{\partial^2\mathbf{E}}{\partial t^2} + \mu\Delta\epsilon\frac{\partial^2\mathbf{E}}{\partial t^2} \tag{7.64}$$

We assume that there are only two significant modes: the incident mode and one diffracted mode. This assumption is called the Bragg assumption and is generally valid at high acoustic frequencies and long interaction lengths. An alternative formulation valid for short interaction lengths and low frequencies results in multiple diffraction orders (analogously to narrowband FM modulation) and is known as the Raman-Nath effect. We do not consider this case. The interaction geometry is shown in Figure 7.5.

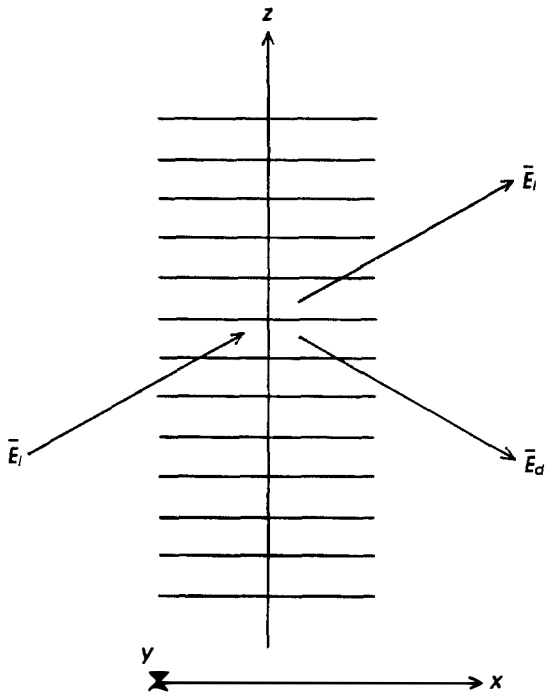

Figure 7.5 Interaction geometry for Bragg diffraction assuming small Bragg angle. Electric field intensity varies only with the x coordinate.

There are two electric fields:

$$\mathbf{E} = \mathbf{E}_i + \mathbf{E}_d \tag{7.65}$$

where

$$\mathbf{E}_i(\mathbf{r}, t) = \tfrac{1}{2}\mathbf{E}_i(\mathbf{r})e^{j(\omega_i t - \mathbf{k}_i \cdot \mathbf{r})} \text{ (incident wave)} \tag{7.66}$$

$$\mathbf{E}_d(\mathbf{r}, t) = \tfrac{1}{2}\mathbf{E}_d(\mathbf{r})e^{j(\omega_d t - \mathbf{k}_d \cdot \mathbf{r})} \text{ (diffracted wave)} \tag{7.67}$$

In (7.66) and (7.67), the spatial variable appears in the field amplitude as well as in the phase. Because we do not assume that the frequencies or propagation vectors of the modes are identical, we allow for the possibility of deflection and frequency-shifting. The acoustic wave (the perturbation in (7.64)) is given by a strain wave (either longitudinal or shear) propagating in the $+z$ direction in an isotropic medium (the anisotropic case will be handled separately).

We further assume that the amplitudes of $\mathbf{E}_i$ and $\mathbf{E}_d$ vary only with x (the deflection angles are usually quite small even at very high frequencies). For the incident wave,

$$\begin{aligned}
\nabla^2\mathbf{E}_i(\mathbf{r}) &= \frac{d^2}{dx^2}\mathbf{E}_i(x, t) \text{ (small-angle approximation)} \\
&= \frac{d}{dx}\left(\frac{d}{dx}\mathbf{E}_i(x, t)\right) \\
&= \frac{1}{2}\frac{d}{dx}\left(\left(\frac{d}{dx}\mathbf{E}_i(x) - j\mathbf{k}_i\right)e^{j(\omega_i t - k_i x)}\right) \\
&= \frac{1}{2}\left(\frac{d^2}{dx^2}\mathbf{E}_i(x) - 2j\mathbf{k}_i\frac{d}{dx}\mathbf{E}_i(x) - k_i^2\mathbf{E}_i(x)\right)e^{j(\omega_i t - k_i x)}
\end{aligned} \tag{7.68}$$

We also assume that the spatial variation of the mode amplitude is slow compared with the optical wavelength; in (7.68),

$$\frac{d^2}{dx^2}E_i(x) \ll k\frac{d}{dx}E_i(x) \tag{7.69}$$

Substituting (7.68) into (7.64) and using (7.69), we have

$$-jk_i\frac{d}{dx}\mathbf{E}_i(x)e^{j(\omega_i t - k_i x)} = \frac{1}{2}[k_i^2 - \omega_i^2\mu\epsilon]\mathbf{E}_i + \mu\Delta\epsilon\frac{d^2}{dt^2}\mathbf{E}_i \tag{7.70}$$

Now,

$$\frac{\omega_i}{k_i} = \frac{1}{\sqrt{\mu\epsilon}}$$

so the term in brackets is zero. An expression similar to (7.70) exists for $\mathbf{E}_d$. Using (7.65), we have for the total electric field:

$$-jk_i \frac{\mathrm{d}}{\mathrm{d}x} \mathbf{E}_i e^{j(\omega_i t - k_i x)} - jk_d \frac{\mathrm{d}}{\mathrm{d}x} \mathbf{E}_d e^{j(\omega_d t - k_d x)} = \mu \Delta\epsilon \frac{\partial^2 \mathbf{E}}{\partial t^2} \tag{7.71}$$

To generate an equation for $\mathbf{E}_i$, we multiply (7.71) by $e^{-j(\omega_i t - k_i x)}$. Equation (7.71) becomes

$$-jk_i \frac{\mathrm{d}}{\mathrm{d}x} \mathbf{E}_i - jk_d \frac{\mathrm{d}}{\mathrm{d}x} \mathbf{E}_d e^{j((\omega_d - \omega_i)t - k_d x)} = \mu \Delta\epsilon \frac{\partial^2 \mathbf{E}}{\partial t^2} e^{-j(\omega_i t - k_i x)} \tag{7.72}$$

The right side of (7.72) contains the acoustic perturbation term $\Delta\epsilon$. Explicitly, this term can be written as

$$\Delta\epsilon = \frac{\Delta\epsilon_a}{2} e^{j(\omega_s t - k_s z)} \tag{7.73}$$

where $\Delta\epsilon_a$ is the wave amplitude, ω_s is the frequency, and k_s is the wave number of the acoustic wave. Note that the acoustic wave propagates in the $+z$ direction. Substituting (7.73) and (7.65) into the right side of (7.72), we obtain

$$\begin{aligned} \Delta\epsilon \mathbf{E} e^{-j(\omega_i t - k_i x)} &= \frac{\Delta\epsilon}{2} e^{j(\omega_s t - k_s z)} e^{-j(\omega_i t - k_i x)} \\ &\quad \cdot \left(\frac{\mathbf{E}_i}{2} e^{j(\omega_i t - k_i x)} + \frac{\mathbf{E}_d}{2} e^{j(\omega_d t - k_d x)} \right) \\ &= \frac{\Delta\epsilon}{4} \left(\mathbf{E}_i e^{j(\omega_s t - k_s z)} \right. \\ &\quad \left. + \mathbf{E}_d e^{j(\omega_s - \omega_i + \omega_d)t} e^{j(k_i x - k_s z - k_d x)} \right) \end{aligned} \tag{7.74}$$

Inspecting (7.74), we note that the first term is a rapidly varying function of time and thus will always average to zero. The time variation of the second term vanishes if

$$\omega_s + \omega_d = \omega_i \tag{7.75}$$

Likewise, the time variation of the second term on the left side of (7.74) vanishes if

$$\omega_i = \omega_d$$

If $\omega_i = \omega_d$, however, the right side of (7.72) is identically zero, and thus there is no variation in either $\mathbf{E}_i$ or $\mathbf{E}_d$. We conclude that the latter term is zero.

Finally, the spatial variation of (7.74) can be written as

$$e^{j(k_i x - k_s z - k_d x)} = e^{j(\mathbf{k}_i \cdot \mathbf{r} - \mathbf{k}_s \cdot \mathbf{r} - \mathbf{k}_d \cdot \mathbf{r})} \tag{7.76}$$

This spatial variation vanishes if

$$\mathbf{k}_i = \mathbf{k}_s + \mathbf{k}_d \tag{7.77}$$

Substituting (7.75) and (7.77) into (7.72), we obtain

$$\frac{d}{dx} E_i = \frac{-j\omega_i^2 \mu \Delta \epsilon E_d}{4k_i} = \frac{-j\omega_i \mu \Delta \epsilon}{4\sqrt{\mu\epsilon}} \tag{7.78}$$

Now,

$$\epsilon = \epsilon_r \epsilon_0 = n^2 \epsilon_0$$

so

$$\frac{d\epsilon}{dn} = 2n\epsilon_0 \quad \text{or} \quad \Delta\epsilon = 2\sqrt{\epsilon_r}\, \epsilon_0 \Delta n \tag{7.79}$$

Substituting (7.79) into (7.78), we get

$$\frac{d}{dx} E_i = \frac{-j\omega_i \mu \sqrt{\epsilon_r}\, \epsilon_0 \Delta n}{2\sqrt{\mu \epsilon_r \epsilon_0}} E_d = \frac{-j\omega_i \sqrt{\mu\epsilon_0}\, \Delta n}{2} E_d \tag{7.80}$$

Because

$$c = \frac{1}{\sqrt{\mu\epsilon_0}}$$

we get

$$\frac{d}{dx} E_i = \frac{-j\omega_i}{2c} \Delta n E_d \tag{7.81}$$

Now, if in (7.71) we multiply by $e^{-j(\omega_d t - k_d x)}$, we derive an equation similar to (7.81) but with E_d replaced by E_i (and *vice versa*). We obtain a set of coupled equations:

$$\frac{d}{dx} E_i = -j\eta E_d \tag{7.82a}$$

$$\frac{d}{dx} E_d = -j\eta E_i \tag{7.82b}$$

where

$$\eta = \frac{\omega_i \Delta n}{2c} \tag{7.83}$$

Equations (7.82a) and (7.82b) describe the spatial evolution of the incident and diffracted optical beams. From (7.75), the frequencies of the two beams differ by the acoustic frequency; i.e., the optical frequency is either up- or downshifted by ω_s, from (7.77), the wave vectors of the two beams differ by the acoustic wave vector; i.e., the diffracted beam is deflected by an angle proportional to the acoustic frequency and velocity, the Bragg angle. In addition, there are polarization rotations due to the possible presence of cross terms in the index ellipsoid.

Differentiating (7.82b) and substituting (7.81a) gives

$$\frac{d^2}{dx^2} E_d = -\eta^2 E_d \tag{7.84}$$

Similarly,

$$\frac{d^2}{dx^2} E_i = -\eta^2 E_i \tag{7.85}$$

The solution of (7.84) is

$$E_d(x) = A \sin\eta x + B \cos\eta x$$

Similarly, for (7.83):

$$E_i(x) = A' \sin\eta x + B' \cos\eta x$$

At $x = 0$:

$$E_d(x) = 0 \rightarrow B = 0$$

Also, from conservation of energy:

$$E_d^2(x) + E_i^2(x) = E_i^2(0) \tag{7.86}$$

so that

$$A' = 0 \text{ and } A = B' = E_i(0)$$

Finally,

$$E_d(x) = E_i(0) \sin\eta x \tag{7.87}$$

$$E_i(x) = E_i(0) \cos\eta x \tag{7.88}$$

From (7.87), we see that the amplitude of the diffracted wave increases sinusoidally as the beams interact with the acoustic wave. This increase is at the expense of the incident wave, which continuously decreases in amplitude. There is an exchange of energy between the two beams that continues until all the energy of the incident beam has been transferred to the diffracted beam. (The complete transfer occurs at $x = \pi/2\eta$.) Further increasing the interaction length (x) or acoustic perturbation ($\Delta\epsilon$) causes the energy to actually transfer back from E_d into E_i.

From (7.87) and (7.83), the ratio of the diffracted intensity to the incident intensity (at small diffracted intensities) is given by

$$\frac{I_{\text{diff}}}{I_{\text{inc}}} = \sin^2\left(\frac{\omega x}{2c}\Delta n\right) \tag{7.89}$$

assuming $\cos^2\eta x \approx 1$. It is useful to express this relation as a function of the power in the acoustic wave. Equation (7.51) relates a mechanical stress to a change in the refractive index:

$$\Delta n = \tfrac{1}{2} n^3 \pi T$$

where π and T are the relevant piezo-optic and stress components. To change the independent variables to the photoelastic constant and strain, we use (7.54):

$$\mathbf{\Pi = p{:}s}$$

and

$$\mathbf{\Pi{:}T = p{:}s{:}c{:}s = p{:}s}$$

Thus,

$$\Delta n = \tfrac{1}{2} n^3 p S \tag{7.90}$$

where S is the strain, which is related to the strain energy density u_S by (1.28):

$$u_S = \tfrac{1}{2} c S^2$$

The intensity of the acoustic wave is

$$I_a = v_a u_S = \frac{v_a}{2} c S^2 = \frac{v_a^3}{2} \rho S^2 \text{ W/m}^2$$

Finally,

$$S = \left(\frac{2 I_a}{\rho v_a^3} \right)^{1/2} \tag{7.91}$$

Substituting (7.91) into (7.89), we get

$$\begin{aligned} \frac{I_{\text{diff}}}{I_{\text{inc}}} &= \sin^2 \left(\frac{\pi x}{\sqrt{2}\,\lambda} n^3 p \left[\frac{I_a}{\rho v_a^3} \right]^{1/2} \right) \\ &= \sin^2 \left(\frac{\pi x}{\sqrt{2}\,\lambda} \left[\frac{n^6 p^2}{\rho v_a^3} \right]^{1/2} I_a^{1/2} \right) \end{aligned} \tag{7.92}$$

In (7.92), λ is the light wavelength in the crystal:

$$\lambda = \frac{\lambda_0}{n} \tag{7.93}$$

The *figure of merit*,

$$M = \frac{n^6 p^2}{\rho v_a^3} \tag{7.94}$$

depends only on the material properties of the crystal and the geometry of the A/O interaction. The density ρ is a property of the crystal only while the refractive index depends on the crystal and the optic wavelength (this dependency is called *dispersion*). The acoustic velocity depends on the particular cut of the crystal and the acoustic mode that is excited (recall that shear mode velocities are usually significantly less than longitudinal velocities). We can determine this velocity by solving the Christoffel equation.

The photoelastic constant is the most difficult part of (7.94) to determine. It depends on the crystal material (the **p** matrix), the crystal orientation with respect to the laser beam, its polarization, and the acoustic mode (longitudinal or shear). We will develop the tools and computer-aided designs later to determine the photoelastic constant for a variety of A/O interaction conditions. It may be argued that a better name for M is the figure of merit for the A/O interaction.

From (7.94), it is clear that the larger the index of refraction the more efficient the interaction (the more light is deflected for a given acoustic power). Because the efficiency also varies as λ^{-2}, shorter optic wavelengths are desirable. Unfortunately, most materials with high refractive index (GaAs, InP, Ge) do not transmit light below about 1 μm. An exception is GaP, which cuts off at about 633 nm (below the HeNe laser wavelength) and possesses an extremely high index (3.3 at 633 nm). For this reason, GaP is an extremely important A/O material. Acoustically, low velocity is important for high A/O efficiency. It would seem reasonable that shear modes should deflect light better than do longitudinal modes. The photoelastic constant of the shear interaction is usually significantly less than that for a longitudinal interaction, however. For an anomalously slow shear mode that occurs, for example, in tellurium dioxide, the effect of the slow velocity completely overwhelms the smaller p components, and the interaction is thus very efficient. Other trade-offs between acoustic velocity, bandwidth, and resolution will be investigated later.

We have previously seen (7.35) that in certain electro-optic interactions and in all photoelastic interactions involving shear stresses the polarization of an incident optic beam is rotated. The angle of rotation depends on the strength of the external field and the magnitude of the relevant electro- or piezo-optic constant. In an A/O interaction, a shear *wave* in, say, a cubic crystal also results in the presence of cross terms in the index ellipsoid. The *deflected* beam is rotated, but at a fixed angle of 90°. Even if the A/O perturbation is weak (short interaction length and

low acoustic intensity), the deflected wave will nevertheless be rotated by 90°. We speak of a shear wave producing a polarization *flipped* interaction.

A polarization flipped interaction is due entirely to the presence of a "cross" term (of the form of (7.35)) in the perturbed index ellipsoid. Thus, it will occur in any symmetry (including isotropic and cubic classes) for shear waves and in trigonal classes for both shear and certain longitudinal waves (due to the presence of p_{14}). Unfortunately, it is quite difficult to prove that a "cross" term in the index ellipsoid results in a polarization flipped interaction. A complete proof would involve not only the index ellipsoid but a vector form of the coupled equations (which contain the optic polarization explicitly). Korpel gives a semiquantitative nonrigorous proof that is relatively easy to follow and provides insight into the nature of the interaction [6].

7.9 WAVE VECTOR DIAGRAMS FOR ACOUSTO-OPTIC INTERACTIONS

A necessary condition for the existence of an A/O interaction is (7.77):

$$\mathbf{k}_i = \mathbf{k}_s + \mathbf{k}_d$$

Equation (7.77) is a statement of the conservation of momentum. Note that (7.77) is a vector equation. For the light beams,

$$|\mathbf{k}_i| = \frac{\omega_i n_i}{c} \quad \text{and} \quad |\mathbf{k}_d| = \frac{\omega_d n_d}{c}$$

The optic frequencies are related by (7.75):

$$\omega_s = \omega_i + \omega_d$$

For a practical device, $\omega_s \approx 10^8$ to 10^{10}, and the optic frequencies are about 10^{15}. Thus, it is clear that the magnitudes of the optic wave vectors are nearly equal if $n_i = n_d$. We differentiate between the incident and diffracted light indices with subscripts, because in a polarization flipped interaction (an acoustic shear wave) in a birefringent medium the two beams will have different indices. The condition that $n_i = n_d$ implies that the medium is isotropic. The wave vector diagram for an A/O interaction in an isotropic medium is illustrated in Figure 7.6. Note that even though the magnitudes of the wave vectors are equal, their directions are not identical.

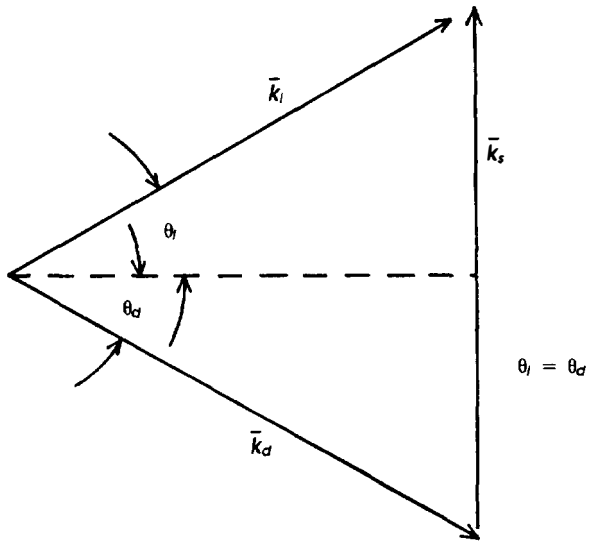

Figure 7.6 Wave vector diagram for the isotropic Bragg interaction. Because the optic frequency is generally so much larger than the acoustic frequency, the magnitudes of the incident and diffracted wave vectors are equal and the triangle is isosceles.

We have

$$|\mathbf{k}_i| = |\mathbf{k}_d| \tag{7.95}$$

So the triangle is isosceles and

$$\theta_i = \theta_d \tag{7.96}$$

The Bragg condition follows immediately from (7.77) and (7.95):

$$k_s = 2k_i \sin(\theta_i) = 2k \sin(\theta_B) \tag{7.97}$$

where θ_B is called the Bragg angle.

Example 7.4: Find the Bragg angle at 1 GHz for a longitudinal ⟨x⟩ $LiNbO_3$ at 633 nm (HeNe).

From (7.97):

$$\sin(\theta_B) = \frac{k_s}{2k} \tag{7.98}$$

The velocity of propagation v_a is determined by solving the Christoffel equation. For the $\langle x \rangle$ longitudinal mode, $v_a = 6.57 \times 10^3$ m/s. Even though $LiNbO_3$ is birefringent, this particular mode does not cause a polarization flip, and thus $n_i = n_d$. We will encounter a longitudinal mode in $LiNbO_3$ that does cause a flip and for which the isotropic theory is not valid. The acoustic wave number is

$$k_s = \frac{\omega_s}{v_a} = \frac{2\pi \times 10^9}{6.57 \times 10^3} = 9.56 \times 10^5 \text{ m}^{-1}$$

The optic wave number is

$$k = \frac{2\pi}{\lambda_0} = 9.9 \times 10^6 \text{ m-}^1$$

and the Bragg angle is (from (7.97))

$$\theta_B = \sin^{-1}\left(\frac{9.56 \times 10^5}{2 \times 9.9 \times 10^6}\right) = 5.5°$$

Note that this is the external Bragg angle and thus does not include the refractive index of lithium niobate. The internal Bragg angle is approximately 2.5°. The geometry of this interaction is shown in Figure 7.7.

7.10 A/O INTERACTION IN A BIREFRINGENT MEDIUM

In an anisotropic crystal, the wave vector diagram, in general, will consist of two optical modes, the ordinary and extraordinary waves. Recall that the ordinary wave is always a circle in the major planes, whereas the extraordinary wave can be a circle or an ellipse, depending on the crystal symmetry and the particular plane. The A/O interaction may occur with either mode, depending on the polarization of the laser. If, however, the interaction flips the laser polarization, then both modes participate. This situation is shown in the wave vector diagram of Figure 7.8. Note that in this case the indices are not equal. Thus the incident and deflected angles as well as the optic wave vector magnitudes are no longer equal.

Our task is to derive relations between the incident and deflected Bragg angles, as functions of acoustic frequency and velocity, and the optic wavelength and indices. Referring to Figure 7.8, we apply the law of cosines to the main triangle:

$$k_s^2 = k_i^2 + k_d^2 - 2k_i k_d \cos(\theta_i + \theta_d)$$

$$k_s^2 = k_i^2 + k_d^2 - 2k_ik_d(\cos\theta_i \cos\theta_d - \sin\theta_i \sin\theta_d) \tag{7.99}$$

From the law of sines,

$$\frac{k_i}{\sin(\pi/2 - \theta_d)} = \frac{k_d}{\sin(\pi/2 - \theta_i)}$$

or

$$\frac{k_i}{\cos(\theta_d)} = \frac{k_d}{\cos(\theta_i)} \tag{7.100}$$

Also, from Figure 7.8(b),

$$\sin(\theta_i) = \frac{a}{k_i} \tag{7.101}$$

$$\sin(\theta_d) = \frac{k_s - a}{k_d} \tag{7.102}$$

Combining (7.101) and (7.102), we get

$$\sin(\theta_i) = \frac{k_s}{k_i} - \frac{k_d}{k_i}\sin(\theta_d) \tag{7.103}$$

Substituting (7.103) and (7.102) into (7.99) gives

$$\begin{aligned} k_s^2 &= k_i^2 + k_d^2 - 2k_ik_d\left\{\cos^2(\theta_d)\frac{k_d}{k_i}\right. \\ &\qquad \left. - \sin(\theta_d)\left[\frac{k_s}{k_i} - \frac{k_d}{k_i}\sin(\theta_d)\right]\right\} \\ &= k_i^2 - k_d^2 - 2\sin(\theta_d)\, k_sk_d \end{aligned} \tag{7.104}$$

Finally,

$$2\sin(\theta_d)k_d = k_s - \frac{k_i^2 - k_d^2}{k_s} \tag{7.105}$$

Solving for $\sin(\theta_i)$ from (7.101) and (7.102), we arrive at

$$2\sin(\theta_i)k_i = k_s + \frac{k_i^2 - k_d^2}{k_s} \tag{7.106}$$

Equations (7.105) and (7.106) are the relations we seek. If the wave numbers are equal, they reduce immediately to the isotropic Bragg equation (7.97).

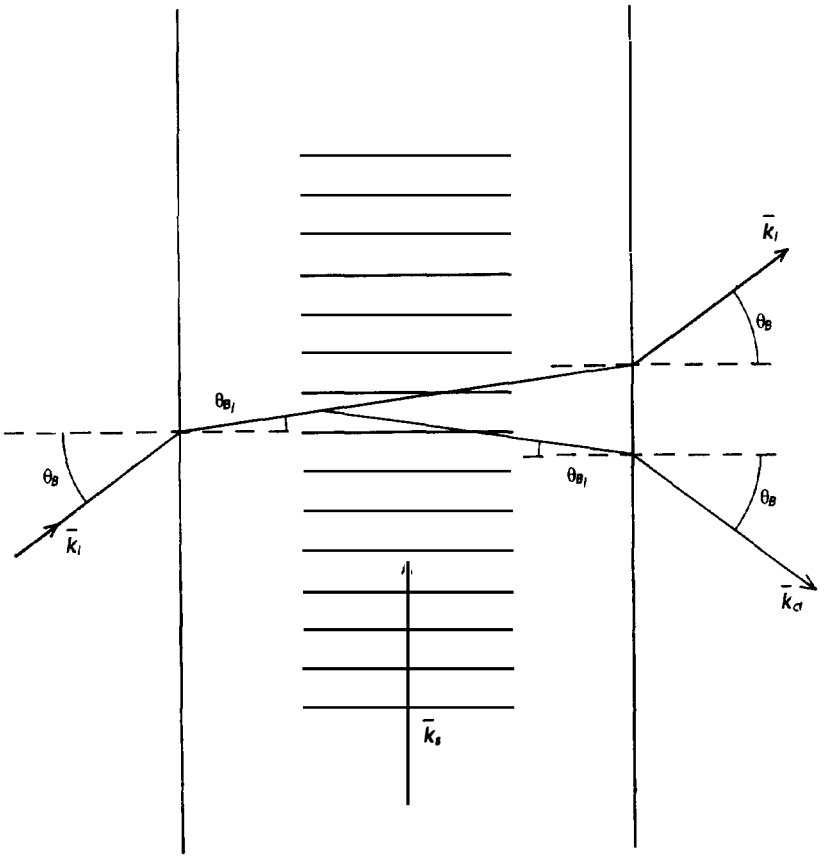

Figure 7.7 Interaction geometry for Example 7.4 showing Snell's law diffraction at the optic interfaces.

We can write Equations (7.105) and (7.106) in a more convenient form, using the simple relations:

$$k_i = \frac{2\pi}{\lambda_0} n_i, \quad k_d = \frac{2\pi}{\lambda_0} n_d, \quad k_s = \frac{2\pi}{\lambda_s}, \quad \lambda_s = \frac{v_a}{f_s}$$

where λ_0 is the free-space optical wavelength and λ_s is the acoustic wavelength. Substituting these relations into (7.105) and (7.106), we obtain

$$\sin(\theta_d) = \frac{\lambda_0}{2n_d v_a}\left[f_s - \frac{v_a^2(n_i^2 - n_d^2)}{f_s\lambda_0^2}\right] \tag{7.107}$$

$$\sin(\theta_i) = \frac{\lambda_0}{2n_i v_a}\left[f_s + \frac{v_a^2(n_i^2 - n_d^2)}{f_s\lambda_0^2}\right] \tag{7.108}$$

The angles θ_i and θ_d are internal angles. To determine the external angles, we multiply (7.107) and (7.108) by n_d and n_i, respectively.

There are two important features of (7.107) and (7.108):

1. There exist maximum and minimum frequencies beyond which no interaction can take place. We can find these frequencies by requiring that

$\sin(\theta_d) = 1$ in(7.107) (maximum interaction frequency)

$\sin(\theta_i) = 1$ in(7.108) (minimum interaction frequency)

Substituting these conditions in (7.107) and (7.108) gives

$$f_s(\max) = \frac{v_a}{\lambda_0}(n_i + n_d) \tag{7.109}$$

$$f_s(\min) = \frac{v_a}{\lambda_0}|n_i - n_d| \tag{7.110}$$

Equation (7.109) is valid for isotropic Bragg diffraction, as we can easily see by requiring that $\sin(\theta) \to 1$ in (7.97):

$$1 = \frac{k_s}{2k_i} = \frac{2\pi f_s/v_a}{4\pi n/\lambda}$$

or

$$f_s = \frac{2v_a n}{\lambda_0}$$

which is identical to (7.109) if we recall that $n = n_i = n_d$ in an isotropic medium. The existence of a maximum frequency places a practical limit on the utility of Bragg deflection devices at very long optical wavelengths.

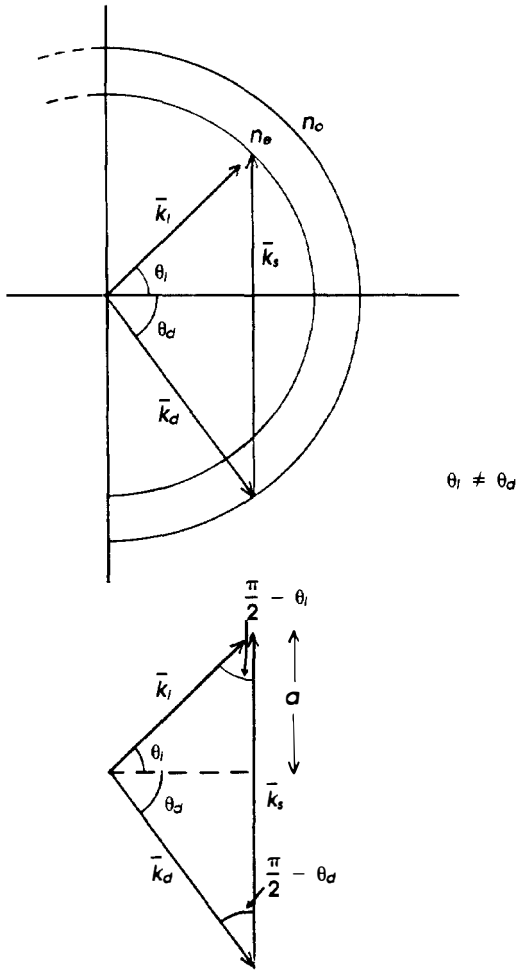

Figure 7.8 Bragg diffraction for birefringent interaction. Because there are two indices, the magnitudes of the optic vectors are not equal and the wave vector diagram is no longer an isosceles triangle.

For example, in fused quartz operating at 10.6 μm (CO_2 laser wavelength), the maximum frequency for a shear acoustic wave is

$$n = 1.5, \quad v_a = 3.8 \times 10^3 \text{ m/s}, \quad f_s \text{ (max)} = 1 \text{ GHz}$$

A significant problem with operation in this region is the nonlinearity of the deflected angle with frequency.

The existence of a minimum frequency is unique to the birefringent interaction. For an important anisotropic interaction in $LiNbO_3$ operating at 633 nm (laser diode),

$$n_i = 2.29, \quad n_d = 2.2, \quad v_a = 3.57 \times 10^3 \text{ m/s}$$

and, from (7.110),

$$f_s \text{ (min)} = .43 \text{ GHz}$$

2. There exists a "critical" frequency about which the incident angle is locally stationary with respect to acoustic frequency. This behavior is in sharp contrast to the isotropic interaction in which the Bragg angle monotonically increases from zero to f_s (max) as the acoustic frequency is increased. We determine the critical frequency by differentiating (7.108) with respect to f_s:

$$\frac{d}{df_s} \sin(\theta_i) = \frac{\lambda_0}{2n_d v_a} \left[1 - \frac{v_a^2(n_i^2 - n_d^2)}{f_s^2 \lambda_0^2} \right] = 0$$

or

$$f_s' = \frac{v_a}{\lambda_0} \sqrt{n_i^2 - n_d^2} \tag{7.111}$$

A consequence of (7.111) is that the optical polarization must be oriented so that the incident refractive index is greater than the diffracted index. Note that f_s' depends on the material properties (the degree of birefringence), the crystal cut (which determines not only the acoustic velocity but also the value of the extraordinary index), and the free-space optic wavelength.

Juggling all of these factors considerably complicates device design and constrains device operation to specific frequency intervals. Additionally, the indices vary appreciably with wavelength (dispersion), which further increases the sensitivity of f_s'. For lithium niobate, for example, $n_o = 2.29$ and $n_e = 2.2$ at 633 nm. If the acoustic phase velocity is 3.5×10^3, we find that the critical frequency is 2.85 GHz. A lithium niobate device utilizing birefringent phase matching is *required* to operate near this center frequency. Curves for lithium niobate are shown in Figure 7.9 for two wavelengths. Note that near the critical frequency the incident

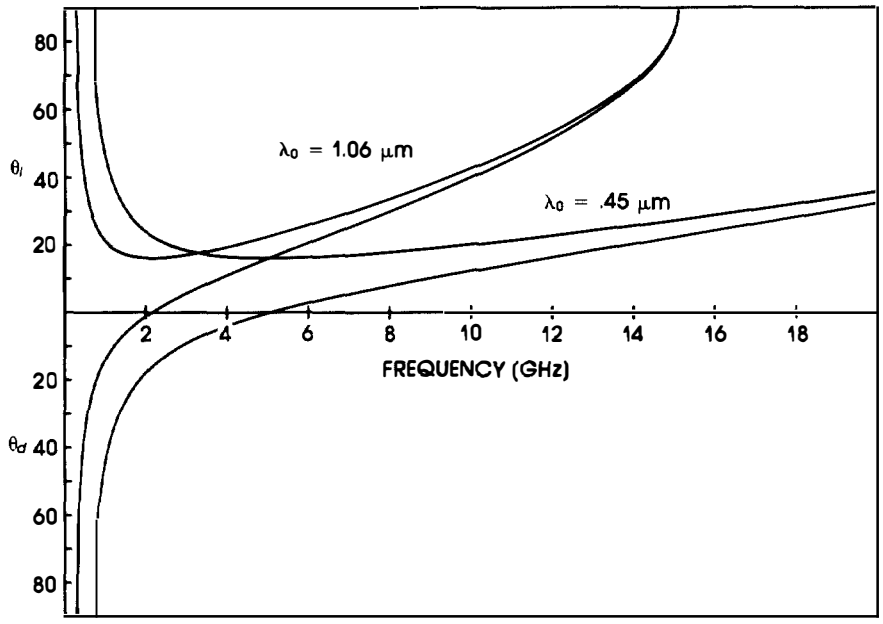

Figure 7.9 Incident and diffracted Bragg angles in a birefringent interaction showing the critical frequency dependence on optic wavelength.

angle is stationary (as predicted by (7.111)), but the diffracted angle increases linearly (it is precisely zero at f_s'). It is this behavior that results in a significant performance advantage, allowing the design of devices with both high deflection efficiency and wide bandwidths.

PROBLEMS

7.1 Show that (7.16) is modified to the equation of a rotated ellipse in the $l_x l_y$ plane if the permittivity matrix contains off-diagonal terms.

7.2 Modify the Christoffel computer program (Figure 3.1) to calculate the phase velocities and inverse velocities of optic modes. Plot the slowness curve of lithium niobate in the yz plane.

7.3 Determine the power flow angle of lithium niobate for the extraordinary mode in the yz plane from the shape of its slowness curve.

7.4 Find the required electric field to produce a birefringence of .001 in GaP, using the electro-optic effect.

7.5 Write the perturbed index ellipsoid for lithium niobate for the following conditions:

$$\mathbf{E} = E_0\hat{\mathbf{i}}$$
$$\mathbf{E} = E_0(\hat{\mathbf{i}} + \hat{\mathbf{j}})$$
$$\mathbf{E} = E_0(\hat{\mathbf{i}} + \hat{\mathbf{k}})$$

7.6 Qualitatively determine the shape of the electro-optically "stiffened" slowness curves of the extraordinary mode of lithium niobate with a z-directed electric field.

7.7 Write the form of the perturbed index ellipsoid in the cubic 23 class (in which $\pi_{12} \neq \pi_{13}$). What are the indices along the principal axes?

REFERENCES

1. M. Born and E. Wolf, *Principles of Optics,* Macmillan, New York, 1964.
2. A. Yariv and P. Yeh, *Optical Waves in Crystals,* John Wiley and Sons, New York, 1984, Chapters 7 to 9.
3. J. Nye, *Physical Properties of Crystals,* Oxford University Press, London, 1957, Chapter 8.
4. N. Uchida and N. Niizeki, "Acoustooptic Deflection Materials and Techniques," *Proc. IEEE* **61** (8) 1073 (1973).
5. J. Sapriel, *Acousto-Optics,* John Wiley and Sons, New York, 1979.
6. A. Korpel, "Acousto-optics." In *Applied Solid State Science,* Vol. 3, R. Wolfe, ed., Academic Press, New York, 1972.
7. M Gottlieb and C. Ireland, *Electro-optic and Acousto-Optic Scanning and Deflection,* Marcel Dekker, New York, 1984.
8. I. Chang, "Acoustooptic Devices and Applications," *IEEE Trans. Sonic Ultrason.* **SU-23** (1), 2 (1976).
9. R. Dixon, "Acoustic Diffraction of Light in Anisotropic Media," *IEEE J. Quantum Electron.* **QE-3** (2), 85 (1967).